A Synopsis of NWS Models for Predicting the Flooding Due to Dam Failures

by D.L. Fread*

April 3,1985

1. INTRODUCTION

Catastrophic flooding occurs when a dam is breached and the impounded water escapes through the breach into the downstream valley. Usually the response time available for warning is much shorter than for precipitation-runoff floods. Dam failures are often caused by overtopping of the dam due to inadequate spillway capacity during large inflows to the reservoir from heavy precipitation runoff. Dam failures may also be caused by seepage or piping through the dam or along internal conduits, slope embankment slides, embankment cracks or liquefaction of earthen dams from earthquakes, and landslide-generated waves within the reservoir. Middlebrooks (1952) describes earthen dam failures occurring within the U.S. prior to 1951. Johnson and Illes (1976) summarize 300 dam failures throughout the world.

During the last decade some major improvements were made in models which predict the changing celerity and magnitude of a flood wave emanating from a breached (failed) dam and propagating through the downstream valley. Such improvements included consideration of the breach dynamics, use of the one-dimensional equations of unsteady flow to route the flood wave through the downstream valley, and consideration of the effects of downstream bridge-embankments, dams, and dead storage areas on the propagating wave.

The National Weather Service (NWS), having the responsibility to advise the public of downstream flooding when there is a failure of a dam, has developed three models to aid NWS hydrologists who are called upon to forecast the extent of flood inundation and available evacuation time. This paper briefly describes the three models (BREACH, DAMBRK, SMPDBK) used to forecast dam-break floods. These models are also used extensively for a multitude of purposes by planners, designers, and analysts who are concerned with possible future flood inundation due to dam-break floods and/or reservoir spillway floods, or any specified flood hydrograph.

Essentially, BREACH can be used to predict the size and timing of the development of the breach in earthen dams. DAMBRK can be used to develop the outflow hydrograph due to a breached dam (earthen or concrete) and determine the extent and timing of the flooding that occurs at various locations downstream of the dam. SMPDBK can do the same thing as DAMBRK except in a relatively simple manner which usually yields more approximate results.

---

*Senior Research Hydrologist, Hydrologic Research Laboratory, National Weather Service, NOAA, 8060 13th Street, Silver Spring, Maryland 20910.

2. BREACH

An earthen dam is subject to possible failure from either overtopping or piping waters which erode a passage (breach) through the dam. The breach formation is gradual with respect to time and its width as measured along the crest of the dam usually encompasses only a portion of the dam's crest length. In many instances, the bottom of the breach progressively erodes downward until it reaches the bottom of the dam; however, in some cases, it may cease its downward progression at some intermediate elevation between the top and bottom of the dam. The size of the breach, as constituted by its depth and its width (which may be a function of the depth), and the rate of the breach formation determine the magnitude and shape of the resulting breach outflow hydrograph. This is of vital interest to hydrologists and engineers concerned with real-time forecasting or evacuation planning for floods produced by dam failures.

BREACH is an enhanced version of a mathematical model (Fread, 1984b) for predicting the breach characteristics (size, shape, time of formation) and the breach outflow hydrograph. The model is physically based on the principles of hydraulics, sediment transport, soil mechanics, the geometric and material properties of the dam, and the reservoir properties (storage volume, spillway characteristics, and time dependent reservoir inflow rate). The dam may be either man-made or naturally formed as a consequence of a landslide. In either, the mechanics of breach formation are very similar, the principal difference being one of scale. The landslide-formed dam is often much larger than even the largest of man-made earthen dams. The critical material properties of the dam are the internal friction angle, cohesion strength, and average grain size diameter (D_{50}).

The BREACH model differs from the parametric approach which the author has used in the NWS DAMBRK Model (Fread, 1977, 1984a). The parametric model uses empirical observations of previous dam failures such as the breach width-depth relation, time of breach formation, and depth of breach to develop the outflow hydrograph. The breach erosion model can provide some advantages over the parametric breach model for application to man-made dams since the critical properties used by the model are measurable or can be estimated within a reasonable range from a qualitative description of the dam materials. However, it should be emphasized that even if the properties can be measured there is a range for their probable value and within this range outflow hydrographs of varying magnitude and shape will be produced by the model. The hydrologist or engineer should investigate the most critical combination of values for the dam's material properties. It is considered essential when predicting breach outflows of landslide dams to utilize a physically based model since observations of such are essentially non-existent, rendering the parametric approach infeasible.

2.1 General Description

The breach erosion model (BREACH) simulates the failure of an earthen dam as shown in Fig. 1. The dam may be homogeneous or it may consist of two materials, an outer zone with distinct material properties (ϕ - friction angle, C - cohesion, D_{50} - average grain size (mm), and γ - unit weight) and an inner core with its ϕ, C, D_{50}, and γ values. Also, the downstream face

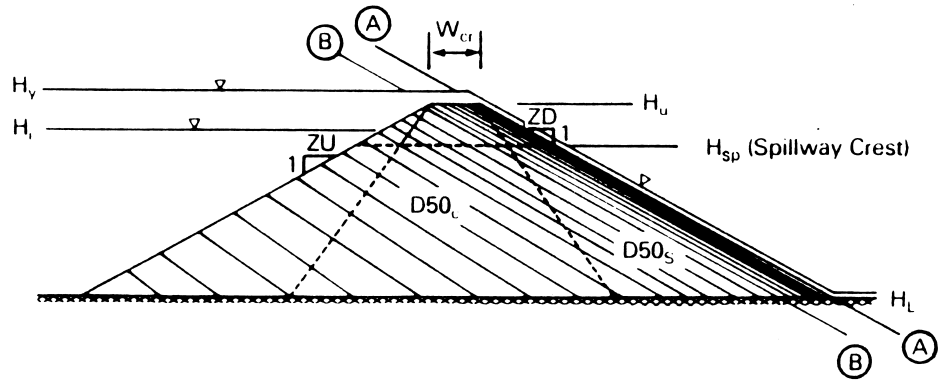

Figure 1. Side View of Dam Showing Conceptualized Overtopping Failure Sequence.

of the dam may be specified as having: 1) a grass cover with specified length of either good or fair stand, 2) material identical to the outer portion of the dam, or 3) material of larger grain size than the outer portion. The geometry of the downstream face of the dam is described by specifying the top of the dam (H_u), the bottom elevation of the dam (H_ℓ) which can also denote the original streambed elevation or the lowest level that the breach will form, and its slope as given by the ratio 1 (vertical) : ZD (horizontal). Then, the geometry of the upstream face of the dam is described by specifying its slope as the ratio 1 (vertical) : ZU (horizontal). If the dam is man-made it is further described by specifying a flat crest width (W_{cr}) and a spillway rating table of spillway flow vs. water elevation, in which the first elevation represents the spillway crest. Naturally formed landslide dams are assumed to not have a flat crest or, of course, a spillway.

The storage characteristics of the reservoir are described by specifying a table of surface area (S_a) in units of acre-ft vs. water elevation, the initial water surface elevation (H_i) at the beginning of the simulation, and a table of reservoir inflows (Q_i) in cfs vs. the hour of their occurrence (T_i).

If an overtopping failure is simulated, the water level (H) in the reservoir must exceed the top of the dam before any erosion occurs. The first stages of the erosion are only along the downstream face of the dam as denoted by the line A-A in Fig. 1 where, initially if no grass cover exists, a small rectangular-shaped rivulet is assumed to exist along the face. An erosion channel of depth-dependent width is gradually cut into the downstream face of the dam. The flow into the channel is determined by the broad-crested weir relationship:

$$Q_b = 3\ B_o(H-H_c)^{1.5} \qquad (1)$$

in which Q_b is the flow into the breach channel, B_o is the instantaneous

width of the initially rectangular-shaped channel, and H_c is the elevation of the breach bottom. As the breach erodes into the downstream face of the dam, the breach bottom elevation (H_c) remains at the top of the dam (H_u), and the most upstream point of the breach channel moves across the crest of the dam towards the dam's upstream face. When the bottom of the erosion channel has attained the position of line B-B in Fig. 1, the breach bottom (H_c) starts to erode vertically downward. The breach bottom is allowed to progress downward until it reaches the bottom elevation of the dam (H_ℓ) or in unusual circumstances to an elevation that may be specified as lower than the bottom of the dam.

If the downstream face of the dam (line A-A in Fig. 1) has a grass cover, the velocity of the overtopping flow along the grassed downstream face is computed at each time step by the Manning equation. This velocity is compared with a specified maximum permissible velocity for grass-lined channels (see Chow, 1959). Failure of the downstream face via erosion is initiated at the time when the permissible velocity is exceeded. At that time a single rivulet having dimensions of one (ft) depth x two width is instantly created along the downstream face. Erosion within the rivulet is allowed to proceed as in the case where a grass cover does not exist. The velocity (v) along the downstream face is computed as follows:

$$q = 3(H-Hc)^{1.5} \tag{2}$$

$$y = \left[\frac{qn'}{1.49(1/ZD)^{0.5}}\right]^{0.6} \tag{3}$$

$$n' = aq^{b} \tag{4}$$

$$v = q/y \tag{5}$$

in which q is the overtopping flow per foot of crest length, (H-Hc) is the hydrostatic head (ft) over the crest, n' is the Manning coefficient for grass-lined channels (Chow, 1959), a and b are fitting coefficients required to represent in mathematical form the graphical curves given in Chow.

If a piping breach is simulated, the initial water level (H) in the reservoir must be greater than the assumed center-line elevation (H_p) of the initially rectangular-shaped piping channel before the size of the pipe starts to increase via erosion. The bottom of the pipe is eroded vertically downward while its top erodes at the same rate vertically upwards. The flow into the pipe is controlled by orifice flow, i.e.,

$$Q_b = A\left[2g(H-Hp)/(1 + fL/D)\right]^{0.5} \tag{6}$$

in which Q_b is the flow (cfs) through the pipe, g is the gravity acceleration constant, A is the cross-sectional area (ft^2) of the pipe channel, (H-Hp) is the hydrostatic head (ft) on the pipe, L is the length (ft) of the

pipe channel, D is the diameter or width (ft) of the pipe, and f is the Darcy friction factor computed from a mathematical representation of the Moody curves (Morris and Wiggert, 1972) and the breach material average grain size (D50). As the top elevation (H_{pu}) of the pipe erodes vertically upward, a point is reached when the flow changes from orifice-control to weir-control. The transition is assumed to occur when the following inequality is satisfied:

$$H < H_{pu} + 2(H_{pu} - H_p) \tag{7}$$

The weir flow is then governed by Eq. (1) in which H_c is equivalent to the bottom elevation of the pipe and B_o is the width of the pipe at the instant of transition. Upon reaching the instant of flow transition from orifice to weir, the remaining material above the top of the pipe and below the top of the dam is assumed to collapse and is transported along the breach channel at the current rate of sediment transport before further erosion occurs. The erosion then proceeds to cut a channel parallel to and along the remaining portion of the downstream face of the dam between the elevation of the bottom of the pipe and the bottom of the dam. The remaining erosion process is quite similar to that described for the overtopping type of failure with the breach channel now in a position similar to line A-A in Fig. 1.

The preceding general description of the erosion process was for a man-made dam. If a landslide dam is simulated the process is identical except, due to the assumption that the landslide dam has no crest width (W_{cr}), the erosion initially commences with the breach channel in the position of line B-B in Fig. 1. A failure mode of overtopping or piping may be initiated for a landslide-formed dam.

2.2 Breach Width

The method of determining the width of the breach channel is a critical component of the breach model. In this model the width of the breach is dynamically controlled by two mechanisms. The first, assumes the breach has an initial rectangular shape as shown in Fig. 2. The width of the breach (B_o) is governed by the following relation:

$$B_o = B_r\, y \tag{8}$$

in which B_r is a factor based on optimum channel hydraulic efficiency and y is the depth of flow in the breach channel. The parameter B_r has a value of 2 for overtopping failures while for piping failures, B_r is set to 1.0. The model assumes that y is the critical depth at the entrance to the breach channel, i.e.,

$$y = 2/3(H-H_c). \tag{9}$$

The second mechanism controlling the breach width is derived from the stability of soil slopes (Spangler, 1951). The initial rectangular-shaped

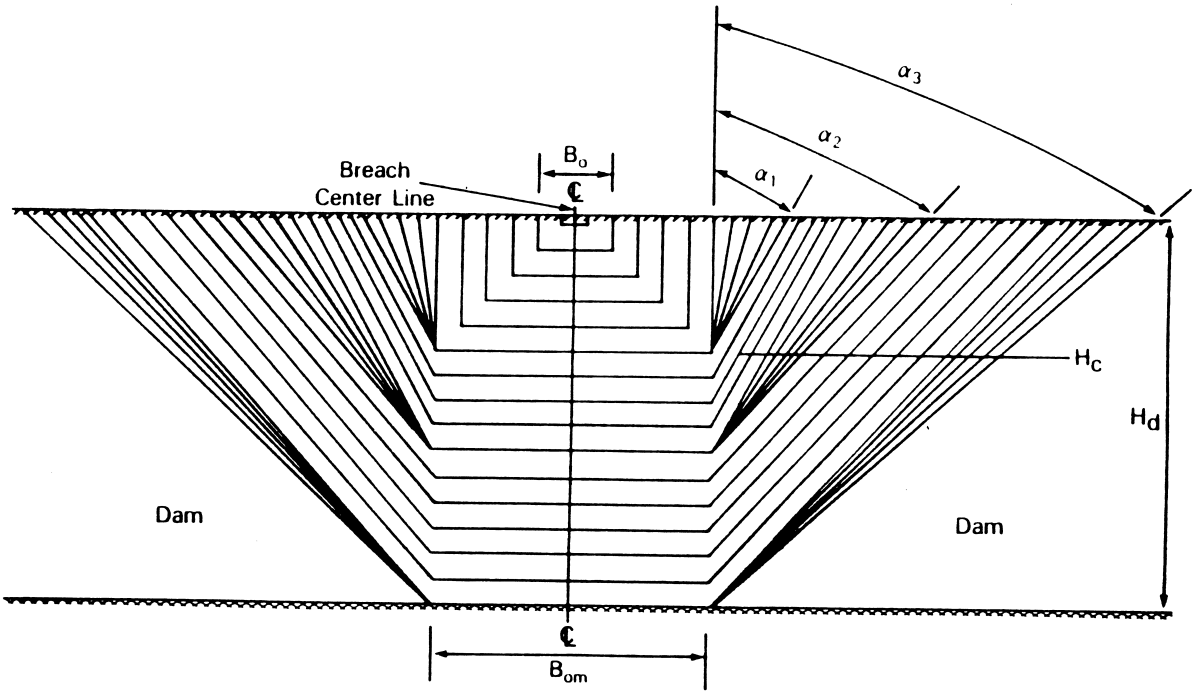

Figure 2. Front View of Dam with Breach Formation Sequence.

channel changes to a trapezoidal channel when the sides of the breach channel collapse, forming an angle (α) with the vertical. The collapse occurs when the depth of the breach cut (H'_c) reaches the critical depth (H') which is a function of the dam's material properties of internal friction (ϕ), cohesion (C), and unit weight (γ), i.e.,

$$H'_k = \frac{4\ C \cos\phi \sin\theta'_{k-1}}{\gamma\ [1 - \cos\ (\theta'_{k-1} - \phi)]} \quad . \ . \ . \quad k = 1,2,3 \tag{10}$$

in which the subscript k denotes one of three successive collapse conditions as shown in Fig. 2, and θ is the angle that the side of the breach channel makes with the horizontal. Angles (θ) and (α) are computed as follows:

$$\Theta = (\Theta'_{k-1} + \phi)/2 \tag{11}$$

$$\alpha = \Pi/2 - \Theta \tag{12}$$

The subscript (k) is incremented by 1 at the instant when

$$H_k > H'_k. \tag{13}$$

where: $H_k = H_c' - y/3$ (14)

The term (y/3) is subtracted from H_c' to give the actual free-standing depth of breach cut in which the supporting influence of the water on the stability of the sides of the breach is taken into account. Through this mechanism, it is possible for the breach to widen after the peak outflow through the breach has occurred since the flow depth (y) diminishes during the receding flow.

Erosion is assumed to occur equally along the bottom and sides of the breach channel except when the sides of the breach channel collapse. Thereupon the breach bottom is assumed not to continue to erode downward until the volume of collapsed material along the breach is removed at the rate of the sediment transport capacity of the breach channel at the instant of collapse. After this characteristically short pause, the breach bottom and sides continue to erode.

2.3 Reservoir Level Determination

Conservation of mass is used to compute the change in the reservoir water surface elevation (H) due to the influence of reservoir inflow (Q_i), spillway outflow (Q_{sp}), crest overflow (Q_o), breach outflow (Q_b), and the reservoir storage characteristics. The conservation of mass over a time step (Δt) in hours is represented by the following:

$$\bar{Q}_i - (\bar{Q}_b + \bar{Q}_{sp} + \bar{Q}_o) = S_a \frac{\Delta H}{\Delta t} \frac{43560}{3600} \tag{15}$$

in which ΔH is the change in water surface elevation during the time interval (Δt), and S_a is the surface area in acres at elevation H. All flows are expressed in units of cfs and the bar (-) indicates the flow is averaged over the time step. Rearranging Eq. (15) yields the following expression for the change in the reservoir water surface:

$$\Delta H = \frac{0.0826 \Delta t}{S_a} (\bar{Q}_i - \bar{Q}_b - \bar{Q}_{sp} - \bar{Q}_o) \tag{16}$$

The reservoir elevation (H) at time (t) can easily be obtained from the relation,

$$H = H' + \Delta H \tag{17}$$

in which H' is the reservoir elevation at time $t-\Delta t$.

The reservoir inflow ($\bar{Q}_i$) is determined from the specified table of inflows (Q_i) vs. time (T_i). The spillway flow ($\bar{Q}_s$) is determined from the specified table of spillway flows (Q_s) vs. reservoir elevation (H). The breach flow (Q_b) is computed from Eq. (6) for piping flow. When the breach flow is weir-type, Eq. (1) is used when $H_c = H_u$; however, when $H_c < H_u$, the following broad-crested weir equation is used:

$$Q_b = 3\ B_o\ (H - H_c)^{1.5} + 2\ \tan(\alpha)\ (H - H_c)^{2.5} \qquad (18)$$

in which B_o is the bottom width and α is given by Eq. (12). The crest overflow is computed as broad-crested weir flow from Eq. (1), where B_o is replaced by the crest length of the dam and H_c is replaced by H_u.

2.4 Breach Channel Hydraulics

The breach flow is assumed to be adequately described by quasi-steady uniform flow as determined by applying the Manning open channel flow equation at each Δt time step, i.e.,

$$Q_b = \frac{1.49\ S^{0.5}\ A^{1.67}}{n\qquad P^{0.67}} \qquad (19)$$

in which S = 1/ZD, A is the channel cross-section area, P is the wetted perimeter of the channel, and n is the Manning coefficient. In this model, n is computed using the Strickler relation which is based on the average grain size of the material forming the breach channel, i.e.,

$$n = 0.013\ D_{50}^{0.167} \qquad (20)$$

in which D_{50} represents the average grain size diameter expressed in mm.

The use of quasi-steady uniform flow is considered appropriate because the extremely short reach of breach channel, very steep channel slopes (1/ZD) for man-made dams, and even in the case of landslide dams where the channel length is greater and the slope is smaller, contribute to produce extremely small variation in flow with distance along the breach channel. The use of quasi-steady uniform flow in contrast to the unsteady flow equations as used by Ponce and Tsivoglou (1981) in their breach erosion model greatly simplifies the hydraulics and computational algorithm. Such simplification is considered commensurate with the other simplifications inherent in the treatment of the breach development in dams for which precise measurements of material properties are lacking or impossible to obtain and the wide variance which exists in such properties in many dams. The simplified hydraulics eliminates troublesome numerical computation problems and enables the breach model to require only minimal computational resources.

2.5 Sediment Transport

The rate at which the breach is eroded depends on the capacity of the flowing water to transport the eroded material. The Meyer-Peter and Muller sediment transport relation as modified by Smart (1984) for steep channels is used, i.e.,

$$Q_s = 3.64\ (D_{90}/D_{30})^{0.2}\ \ \frac{D^{2/3}}{n}\ \ S^{1.1}\ (DS - 0.0054\ D_{50}\ \tau_c) \qquad (21)$$

where:

$$\tau_c = a' \tau_c' \quad (22)$$

$$a' = \cos \theta (1. - 1.54 \tan \theta) \quad (23)$$

$$\theta = \tan^{-1} S \quad (24)$$

$$\tau_c' = 10^{-1.21 - .19 \log R^*} \quad \ldots\ldots\ldots\ldots R^* < 30 \quad (25)$$

$$\tau_c' = 10^{-1.49 + .35(\log R^* - 1.48)} \quad \ldots\ldots\ldots 30 \leq R^* \leq 200 \quad (26)$$

$$\tau_c' = 0.062 \quad \ldots\ldots\ldots 200 < R^* < 25000 \quad (27)$$

$$S = \frac{1}{ZD} \quad (28)$$

$$R^* = 1524 \; D_{50} \; (DS)^{0.5} \quad (29)$$

in which Q_s is the sediment transport rate (cfs); D_{30}, D_{50}, D_{90} (mm) are grain sizes at which 30, 50, and 90 percent of the total weight is finer; D is the hydraulic depth of flow (ft), S is the slope of the downstream face of the dam; and τ_c' is the Shields' critical shear stress.

2.6 Breach Enlargement By Sudden Collapse

It is possible for the breach to be enlarged by a rather sudden collapse failure of the upper portions of dam in the vicinity of the breach development. Such a collapse would consist of a wedge-shaped portion of the dam having a vertical dimension (Y_c). The collapse would be due to the pressure of the water on the upstream face of the dam exceeding the resistive forces due to shear and cohesion which keep the wedge in place. When this occurs the wedge is pushed into the breach and then transported by the escaping water through the now enlarged breach. When collapse occurs, the erosion of the breach ceases until the volume of the collapsed wedge is transported through the breach channel at the transport rate of the water escaping through the suddenly enlarged breach. A check for collapse is made at each Δt time step during the simulation. The collapse check consists of summing the forces acting on the wedge of height, Y_c. The forces are those due to the water pressure and the resisting forces which are the shear force acting along the bottom of the wedge, the shear force acting along both sides of the wedge, the force due to cohesion along the sides and bottom of the wedge.

2.7 Computational Algorithm

The sequence of computations in the model are iterative since the flow into the breach is dependent on the bottom elevation of the breach and its width while the breach properties are dependent on the sediment transport capacity of the breach flow; the transport capacity is dependent on the breach size and flow. A simple iterative algorithm is used to account for the mutual dependence of the flow, erosion, and breach properties. An estimated incremental erosion depth ($\Delta H'_c$) is used at each time step to start the iterative computation. This estimated value can be extrapolated from previously computed incremental erosion depths after the first few time steps. The computational algorithm is described elsewhere (Fread, 1984b).

2.8 Computational Requirements

The basic time step (Δt) is specified; however when rapid erosion takes place the basic time step is automatically reduced to $\Delta t/20$. The specified value for the basic time step is usually about 0.02 hrs with slightly larger values acceptable for landslide dams. For typical applications, the BREACH model requires less than 10 seconds of CPU time on a Prime 750 computer and less than 2 seconds on an IBM 360/195 computer, both of which are mainframe computers. Although it has not been used on microcomputers, it would be quite amenable to such applications.

The model has displayed a lack of numerical instability or convergence problems. The computations show very little sensitivity to a reasonable variation in basic time step size. Numerical experimentation indicates that as the time step is increased by a factor of 4, the computed peak flow (Q_p), time of peak (T_p), and final breach dimensions vary by less than 10, 4, and 0.5 percent, respectively.

2.9 Model Applications

The BREACH model was applied to two earthen dams to determine the outflow hydrograph produced by a gradual breach of each. The first was the piping failure of the man-made Teton dam in Idaho, and the second was an overtopping failure of the landslide-formed dam which blocked the Mantaro River in Peru.

2.9.1 Teton Dam

The Teton Dam, a 300 ft high earthen dam with a 3000 ft long crest and 262 ft depth of stored water amounting to about 250,000 acre-ft, failed on June 5, 1976. According to a report by Ray, et. al (1976) the failure started as a piping failure about 10:00 AM and slowly increased the rate of outflow until about 12:00 noon when the portion of the dam above the piping hole collapsed and in the next few minutes (about 12 minutes according to Blanton (1977)) the breach became fully developed allowing an estimated 1.6 to 2.8 million cfs (best estimate of 2.3) peak flow (Brown and Rogers, 1977) to be discharged into the valley below. At the time of peak flow the breach was estimated from photographs to be trapezoidal shape having a top width at

the original water surface elevation of about 500 ft and side slopes of about 1 vertical to 0.5 horizontal. After the peak outflow the outflow gradually decreased to a comparatively low flow in about five hours as the reservoir volume was depleted and the surface elevation receded. The downstream face of the dam had a slope of 1:2 and the upstream face 1:2.5. The crest width was 35 ft and the bulk of the breach material was a D_{50} size of 0.03 mm. The inflow to the reservoir during failure was insignificant and the reservoir surface area at time of failure was about 1950 acre-ft.

The BREACH model was applied to the piping generated failure of the Teton Dam. The center-line elevation for the piping breach was 160 ft above the bottom of the dam, and an initial width of 0.1 ft was used for the assumed square-shaped pipe. The material properties of the breach were assumed as follows: ϕ = 40 deg, C = 250 lb/ft^2, and γ = 100 lb/ft^3. The Strickler equation was judged not to be applicable for the extremely fine breach material, and the n value was computed as 0.013 from a Darcy friction factor based on the D_{50} grain size and the Moody curves. The computed outflow hydrograph is shown in Fig. 3. The timing, shape, and magnitude of the hydrograph compares quite well with the estimated actual values. The computed peak outflow of 2.3 million cfs agrees with the best estimate made by the U.S. Geological Survey and the time of occurrence is also the same. The computed breach width of 460 ft agrees closely with the estimated value

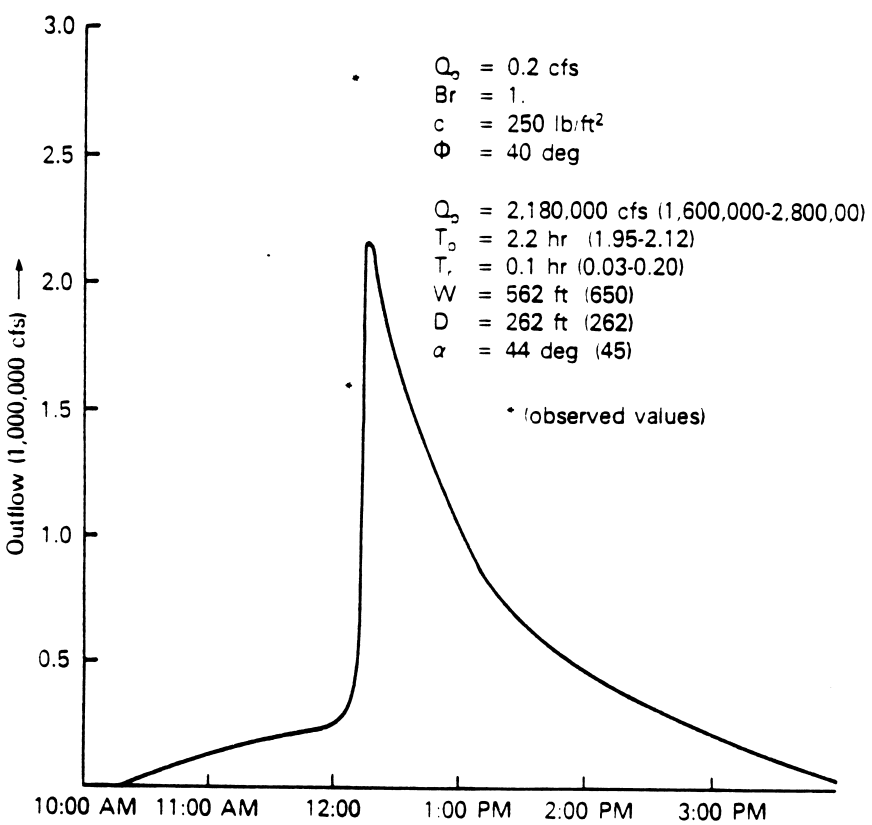

Figure 3. Teton Dam: Predicted and Observed Breach Outflow Hydrograph and Breach Properties.

of 500 ft at the elevation of the initial reservoir water surface. A larger estimated actual breach width of 650 ft breach width was reported by Brown and Rogers (1977); however this was the final breach width after additional enlargement of the breach occurred. The (BREACH) model produced a final width of 560 ft when the reservoir water elevation had receded to near the reservoir bottom; the additional widening of the breach during the recession of the outflow is due to the influence of the depth (y) in Eq. (14).

Sensitivities of the peak breach outflow (Q_p), time of peak flow (T_p) and the top width (W) of the trapezoidal-shaped breach to variations in the specified breach material properties, cohesive strength (C) and internal friction angle (ϕ), are shown in Fig. 4. The dashed lines apply to the Teton simulation. Peak outflow is moderately affected by the cohesion; however it is sensitive to the ϕ value which mostly controls the enlargement of the breach width. Q_p is sensitive to a full range of ϕ values, however the ϕ value may vary by ± 10 degrees with less than 20% variation in Q_p. The breach width (W) was moderately sensitive to variations in the cohesion (C), and somewhat more sensitive to the ϕ value. The time to peak outflow (T_p) was almost insensitive to variations in C and ϕ .

2.9.2 Mantaro Landslide Dam

A massive landslide occurred in the valley of the Mantaro River in the mountainous area of central Peru on April 25, 1974. The slide, with a volume of approximately 5.6×10^{10} ft^3, dammed the Mantaro River and formed

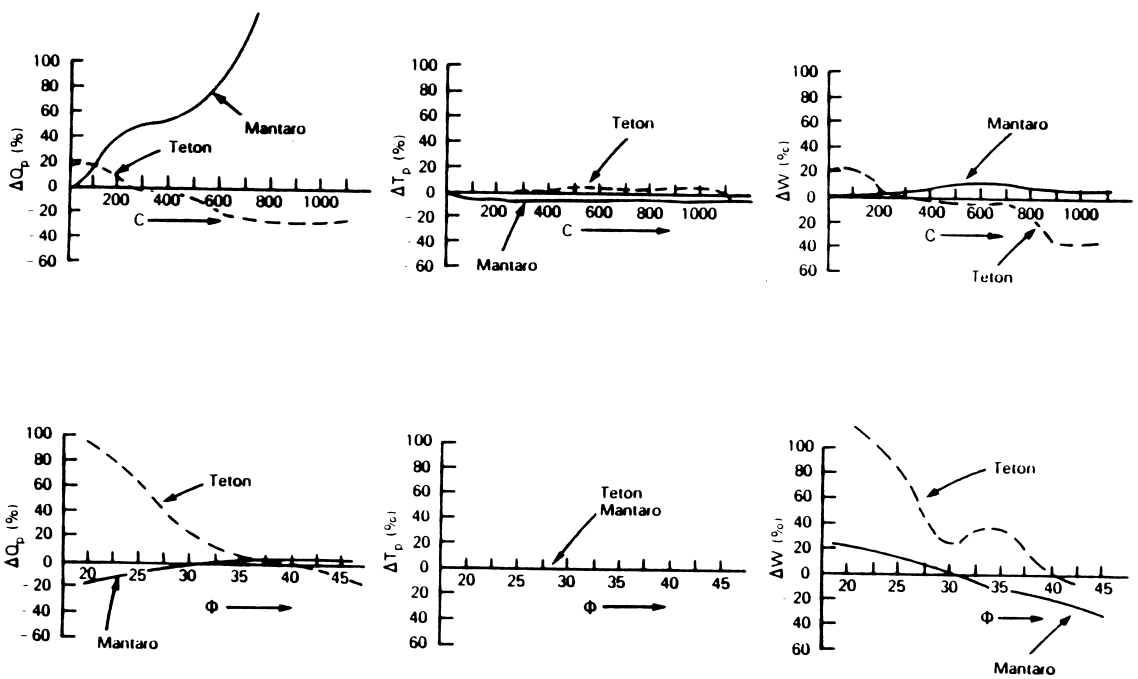

Figure 4. Sensitivity of Mantaro and Teton Predictions of Peak Outflow (Q_p), Time to Peak (T_p), and Breach Width (W) to Changes in the Material Properties of the Dam: Cohesion (C) and Internal Friction Angle (Φ).

a lake which reached a depth of about 560 ft before overtopping during the period June 6-8, 1974 (Lee and Duncan, 1975). The overtopping flow very gradually eroded a small channel along the approximately 1-mile long downstream face of the slide during the first two days of overtopping. Then a dramatic increase in the breach channel occurred during the next 6-10 hrs resulting in a final trapezoidal-shaped breach channel approximately 350 ft in depth, a top width of some 800 ft, and side slopes of about 1:1. The peak flow was estimated at 353,000 cfs as reported by Lee and Duncan (1975), although Ponce and Tsivoglou (1981) later reported an estimated value of 484,000 cfs. The breach did not erode down to the original river bed; this caused a rather large lake to remain after the breaching had subsided some 24 hrs after the peak had occurred. The slide material was mostly a mixture of silty sand with some clay resulting in a D_{50} size of about 11 mm with some material ranging in size up to 3-ft boulders.

The BREACH model was applied to the Mantaro landslide-formed dam using the following parameters: ZU = 17, ZD = 8.0, H_u = 560 ft, D_{50} = 11 mm, P_{or} = 0.5, S_a = 1200 acres, C = 30 lb/ft^2, ϕ = 30 deg, γ = 100 lb/ft^3 B_r = 2, and Δt = 0.1 hr. The Manning n was estimated by Eq. (20) as 0.020 and the initial breach depth was assumed to be 0.3 ft. The computed breach outflow is shown in Fig. 5 along with the estimated actual values. The timing of the peak outflow and its magnitude are very similar except for a somewhat more gradual rising limb of 10 hr compared to the estimated actual of 6 hr. The dimensions of the gorge eroded through the dam are similar as shown by the values of D, W, and α in Fig. 5.

The sensitivities of Q_p, T_p and W for variations in C and ϕ are shown in Fig. 4. The solid line denotes the Mantaro application. Most notably, Q_p is very sensitive to the cohesion (C) while much less sensitive to the internal friction angle (ϕ). T_p is almost insensitive to the value of C and quite insensitive to ϕ. W is not very sensitive to C and moderately sensitive to ϕ; a variation of $\pm$ 10 degrees in ϕ results in a change in W of less than 20%.

3. DAMBRK

The DAMBRK model represents the current state-of-the-art in understanding of dam failures and the utilization of hydrodynamic theory to predict the dam-break wave formation and downstream progression. The model has wide applicability; it can function with various levels of input data ranging from rough estimates to complete data specification; the required data is readily accessible; and it is economically feasible to use, i.e., it requires a minimal computation effort on mainframe computing facilities and can be used with microcomputers.

The model consists of three functional parts, namely: (1) description of the dam failure mode, i.e., the temporal and geometrical description of the breach; (2) computation of the time history (hydrograph) of the outflow through the breach as affected by the breach description, reservoir inflow, reservoir storage characteristics, spillway outflows, and downstream

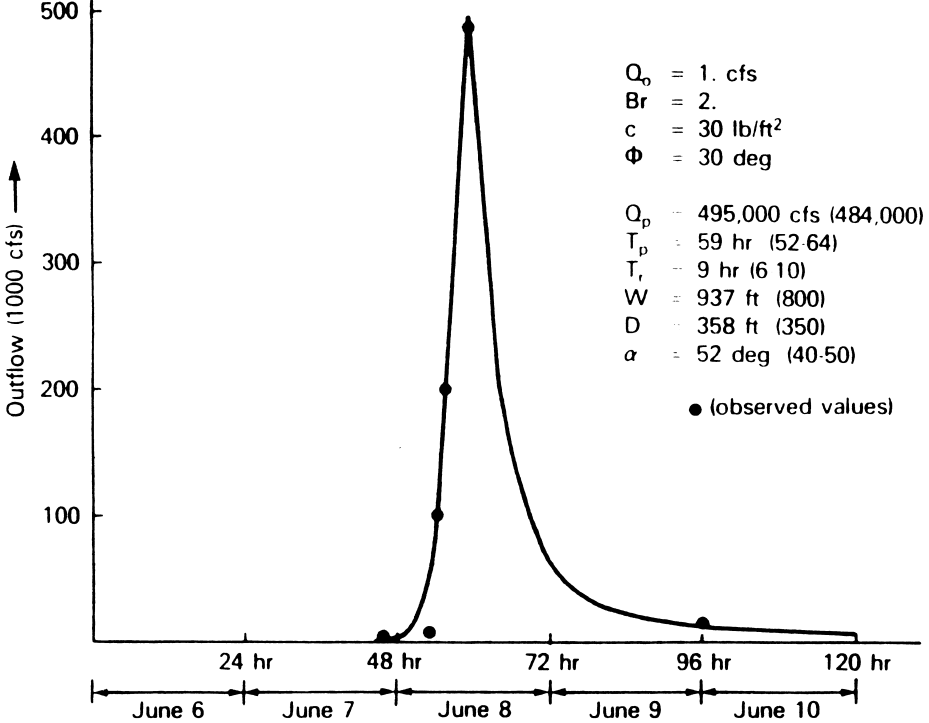

Figure 5. Mantaro Landslide Dam: Predicted and Observed Breach Outflow Hydrograph and Breach Properties.

tailwater elevations; and (3) routing of the outflow hydrograph through the downstream valley in order to determine the changes in the hydrograph due to valley storage, frictional resistance, downstream bridges or dams, and to determine the resulting water surface elevations (stages) and flood-wave travel times.

DAMBRK is an expanded version of a practical operational model first presented in 1977 by the author (Fread, 1977). That model was based on previous work by the author on modeling breached dams (Fread and Harbaugh, 1973) and routing of flood waves (Fread, 1974a, 1976).

3.1 Breach Description

The breach is the opening formed in the dam as it fails. Earthen dams which exceedingly outnumber all other types of dams do not tend to completely fail, nor do they fail instantaneously. The fully formed breach in earthen dams tends to have an average width ($\bar{b}$) in the range ($h_d < \bar{b} < 4h_d$) where h_d is the height of the dam. The middle portion of this range for $\bar{b}$ is supported by the summary report of Johnson and Illes (1976). Breach widths for earthen dams are therefore usually much less than the total length of the dam as measured across the valley. Also, the breach requires a finite interval of time for its formation through erosion of the dam materials by the escaping water. Total time of failure may be in the range of a few minutes to a few hours, depending on the height of the dam, the type materials used in construction, the extent of compaction of the

materials, and the extent (magnitude and duration) of the overtopping flow of the escaping water. Piping failures occur when initial breach formation takes place at some point below the top of the dam due to erosion of an internal channel through the dam by escaping water. As the erosion proceeds, a larger and larger opening is formed; this is eventually hastened by caving-in of the top portion of the dam.

Concrete gravity dams also tend to have a partial breach as one or more monolith sections formed during the construction of the dam are forced apart by the escaping water. The time for breach formation is in the range of a few minutes.

Poorly constructed earthen dams and coal-waste slag piles which impound water tend to fail within a few minutes, and have average breach widths in the upper range or even greater than those for the earthen dams mentioned above.

In DAMBRK, the failure time (τ) and the size and shape of the breach are selected as input parameters similar to the approach used by Fread and Harbaugh (1973). The shape (see Fig. 6) is specified by a parameter (z) identifying the side slope of the breach, i.e., 1 vertical: z horizontal slope. The range of z values is: $0 \leq z \leq 2$. Rectangular triangular, or trapezoidal shapes may be specified in this way. For example, z=0 and b>0 produces a trapezoidal shape. The final breach size is controlled by the z parameter and another parameter (b) which is the terminal width of the bottom of the breach. As shown in Fig. 6, the model assumes the breach bottom width starts at a point and enlarges at a linear rate over the failure time interval (τ) until the terminal width is attained and the breach bottom has eroded to the elevation h_{bm} which is usually, but not necessarily, the bottom of the reservoir or outlet channel bottom. If τ is less than 10 minutes, the width of the breach bottom starts at a value of b rather than at a point. This represents more of a collapse failure than an erosion failure.

During the simulation of a dam failure, the actual breach formation commences when the reservoir water surface elevation (h) exceeds a specified value, h_f. This feature permits the simulation of an overtopping of a dam in which the breach does not form until a sufficient amount of water is flowing over the crest of the dam. A piping failure may be simulated when h_f is specified less than the height of the dam, h_d.

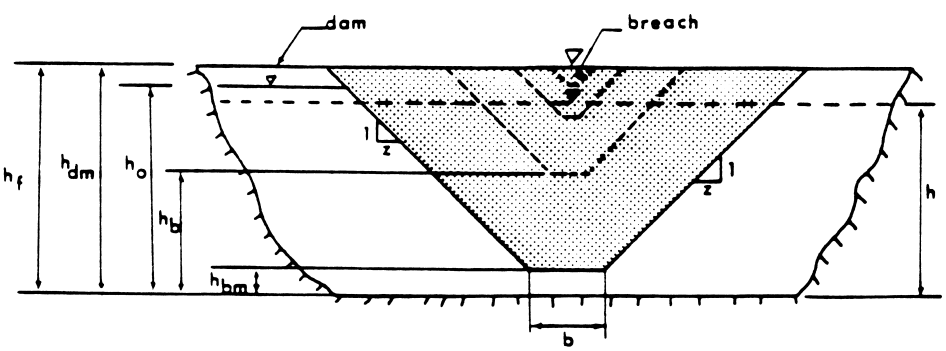

Figure 6. Front View of Dam Showing Formation of Breach

Selection of breach parameters before a breach forms, or in the absence of observations, introduces a varying degree of uncertainty in the model results; however, errors in the breach description and thence in the resulting time rate of volume outflow are rapidly damped-out as the flood wave advances downstream. For conservative forecasts which err on the side of larger flood waves, values for b and z should produce an average breach width ($\bar{b}$) in the uppermost range for a certain type of dam. Failure time (τ) should be selected in the lower range to produce a maximum outflow.

3.2 Reservoir Outflow Hydrograph

The total reservoir outflow consists of broad-crested weir flow through the breach and flow through any spillway outlets, i.e.,

$$Q = Q_b + Q_s \tag{30}$$

The breach outflow (Q_b) is computed as:

$$Q_b = c_1(h-h_b)^{1.5} + c_2(h-h_b)^{2.5} \tag{31}$$

where:

$$c_1 = 3.1\ b_i\ c_v\ k_s \tag{32}$$

$$c_2 = 2.45\ z\ c_v\ k_s \tag{33}$$

$$h_b = h_d - (h_d-h_{bm})\ \frac{t_b}{\tau} \qquad \text{if} \qquad t_b \leq \tau \tag{34}$$

$$h_b = h_{bm} \qquad \text{if} \qquad t_b > \tau \tag{35}$$

$$b_i = b\ t_b/\tau \qquad \text{if} \qquad t_b \leq \tau \tag{36}$$

$$c_v = 1.0 + 0.023\ Q^2/[B_d^2\ (h-h_{bm})^2\ (h-h_b)] \tag{37}$$

$$k_s = 1.0 \qquad \text{if} \qquad \frac{h_t-h_b}{h-h_b} \leq 0.67 \tag{38}$$

otherwise:

$$k_s = 1.0 - 27.8\ \left[\frac{h_t-h_b}{h-h_b} - 0.67\right]^3 \tag{39}$$

in which h_b is the elevation of the breach bottom, h is the reservoir water surface elevation, b_i is the instantaneous breach bottom width, t_b is time

interval since breach started forming, c_v is correction for velocity of approach, Q is the total outflow from the reservoir, B_d is width of the reservoir at the dam, k_s is the submergence correction for tailwater effects on weir outflow (Venard, 1954), and h_t is the tailwater elevation (water surface elevation immediately downstream of dam).

The tailwater elevation (h_t) is computed from Manning's equation, i.e.,

$$Q = \frac{1.49}{n} S^{1/2} \frac{A^{5/3}}{B^{2/3}} \tag{40}$$

in which n is the Manning roughness coefficient, A is the cross-sectional area of flow, B is the top width of the wetted cross-sectional area, and S is the energy slope. Each term in Eq. (40) applies to a representative channel reach immediately downstream of the dam. The S parameter can be specified by the user; it does not change with time; if it is not specified, the model uses the channel bottom slope of the first third of the downstream valley reach. Since A and B are functions of h_t and Q is the total discharge given by Eq. (30), Eq. (40) provides a sufficiently accurate value for h_t if there are no backwater effects immediately below the dam due to downstream constrictions, dams, bridges, or significant tributary inflows. When these affect the tailwater, Eq. (40) is not used and the dam is treated as an internal boundary which is described in a following section on multiple dams and bridges.

If the breach is formed by piping, Eq. (31)-(39) are replaced by the following orifice flow equation:

$$Q_b = 4.8 A_p (h-\bar{h})^{1/2} \tag{41}$$

where:

$$A_p = [2b_i+4z(h_f-h_b)] (h_f-h_b) \tag{42}$$

$$\bar{h} = h_f \quad \text{if} \quad h_t \leq 2h_f - h_b \tag{43}$$

$$\bar{h} = h_t \quad \text{if} \quad h_t > 2h_f - h_b \tag{44}$$

and h_d is replaced by h_f in Eq. (34) to compute h_b. However, if $\bar{h} = h_f$ and

$$h - h_b < 2.2(h_f-h_b) \tag{45}$$

the flow ceases to be orifice flow and the broad-crested weir flow, Eq. (31), is used.

The spillway outflow (Q_s) is computed as:

$$Q_s = c_s L_s (h-h_s)^{1.5} + c_g A_g (h-h_g)^{0.5} + c_d L_d (h-h_d)^{1.5} + Q_t \qquad (46)$$

in which c_s is the uncontrolled spillway discharge coefficient, h_s is the uncontrolled spillway crest elevation, c_g is the gated spillway discharge coefficient, h_g is the center-line elevation of the gated spillway, c_d is the discharge coefficient for flow over the crest of the dam L_s is the spillway length, A_g is the gate flow area, L_d is the length of the dam crest less L_s, and Q_t is a constant outflow term which is head independent. The uncontrolled spillway flow or the gated spillway flow can also be represented as a table of head-discharge values. The gate flow may also be specified as a function of time.

The total outflow is a function of the water surface elevation (h). Depletion of the reservoir storage volume by the outflow causes a decrease in h which then causes a decrease in Q. However, any inflow to the reservoir tends to increase h and Q. In order to determine the total outflow (Q) as function of time, the simultaneous effects of reservoir storage characteristics and reservoir inflow require the use of a reservoir routing technique. DAMBRK utilizes a hydrologic storage routing technique based on the law of conservation of mass, i.e.,

$$I - Q = dS/dt \qquad (47)$$

in which I is the reservoir inflow, Q is the total reservoir outflow, and dS/dt is the time rate of change of reservoir storage volume. Eq. (47) may be expressed in finite difference form as:

$$(I+I')/2 - (Q+Q')/2 = \Delta S/\Delta t \qquad (48)$$

in which the prime (') superscript denotes values at the time $t-\Delta t$ and the Δ approximates the differential. The term ΔS may be expressed as:

$$\Delta S = (A_s+A_s') (h-h')/2 \qquad (49)$$

in which A_s is the reservoir surface area coincident with the elevation (h).

Combining Eqs. (30), (31), (46), (48) and (49) result in the following expression:

$$(A_s+A_s') (h-h')/\Delta t + c_1(h-h_b)^{1.5} + c_2(h-h_b)^{2.5} + c_s(h-h_b)^{1.5}$$

$$+ c_g(h-h_g)^{0.5} + c_d(h-h_d)^{1.5} + Q_t + Q' - I - I' = 0 \qquad (50)$$

Since A_s is a function of h and all other terms except h are known, Eq. (50) can be solved for the unknown h using Newton-Raphson iteration. Once h is

obtained, Eqs. (31) and (46) can be used to obtain the total outflow (Q) at time (t). In this way the outflow hydrograph Q(t) can be developed for each time (t) as to goes from zero to some terminating value (t_e) sufficiently large for the reservoir to be drained. In Eq. (50) the time step (Δt) is chosen sufficiently small to incur minimal numerical integration error. This value is preset in the model to $\tau/50$.

3.3 Downstream Routing

After computing the hydrograph of the reservoir outflow, the extent of and time of occurrence of flooding in the downstream valley is determined by routing the outflow hydrograph though the valley. The hydrograph is modified (attenuated, lagged, and distorted) as it is routed through the valley due to the effects of valley storage, frictional resistance to flow, and downstream obstructions and/or flow control structures. Modifications to the dam-break flood wave are manifested as attenuation of the flood peak elevation, spreading-out or dispersion of the flood wave volume, and changes in the celerity (translation speed) or travel time of the flood wave. If the downstream valley contains significant storage volume such as a wide flood plain, the flood wave can be extensively attenuated and its time of travel greatly increased. Even when the downstream valley approaches that of a uniform rectangular-shaped section, there is appreciable attenuation of flood peak and reduction in wave celerity as the wave progresses through the valley.

A distinguishing feature of dam-break waves is the great magnitude of peak discharge when compared to runoff-generated flood waves having occurred in the past in the same valley. The dam-break flood is usually many times greater than the runoff flood of record. The above-record discharges make it necessary to extrapolate certain coefficients used in various flood routing techniques and make it impossible to fully calibrate the routing technique.

Another distinguishing characteristic of dam-break floods is the very short duration time, and particularly the extremely short time from beginning of rise until the occurrence of the peak. The time to peak is in almost all instances synonymous with the breach formation time (τ) and, therefore, is in the range of a few minutes to a few hours. This feature, coupled with the great magnitude of the peak discharge, causes the dam-break flood wave to have acceleration components of a far greater significance than those associated with a runoff-generated flood wave.

A hydraulic routing technique (dynamic routing) based on the complete equations of unsteady flow is used to route the dam-break flood hydrograph through the downstream valley. This method is derived from the original equations developed by Barre De Saint-Venant (1871). In this method the important acceleration effects are properly considered. Also, the only coefficient that must be extrapolated beyond the range of past experience is the coefficient of flow resistance. It so happens that this is usually not a sensitive parameter in effecting the modifications of the flood wave due to its progression through the downstream valley. The dynamic routing technique properly considers the effect of downstream constrictions and flow control structures such as bridge-road embankments or dams.

The Saint-Venant unsteady flow equations consist of a conservation of mass equation, i.e.,

$$\frac{\partial Q}{\partial x} + \frac{\partial (A+A_o)}{\partial t} - q = 0 \tag{51}$$

and a conservation of momentum equation, i.e.,

$$\frac{\partial Q}{\partial t} + \frac{\partial (Q^2/A)}{\partial x} + gA\left(\frac{\partial h}{\partial x} + S_f + S_e\right) + L = 0 \tag{52}$$

where A is the active cross-sectional area of flow, A_o is the inactive (off-channel storage) cross-sectional area, x is the longitudinal distance along the channel (valley), t is the time, q is the lateral inflow or outflow per linear distance along the channel (inflow is positive and outflow is negative in sign), g is the acceleration due to gravity, S_f is the friction slope, and S_e is the expansion-contraction slope. The friction slope is evaluated from Manning's equation for uniform, steady flow, i.e.,

$$S_f = \frac{n^2 |Q| Q}{2.21\ A^2\ R^{4/3}} \tag{53}$$

in which n is the Manning coefficient of frictional resistance and R is the hydraulic radius defined as A/B where B is the top width of the active cross-sectional area. The term (S_e) is defined as follows:

$$S_e = \frac{k\ \Delta (Q/A)^2}{2g\ \Delta x} \tag{54}$$

in which k (Morris and Wiggert, 1972) is the expansion-contraction coefficient varying from 0.0 to ±1.0 (+ if contraction, - if expansion), and $\Delta(Q/A)^2$ is the difference in the term $(Q/A)^2$ at two adjacent cross-sections separated by a distance Δx. L is the momentum effect of lateral flow assumed herein to enter or exit perpendicular to the direction of the main flow. This term has the following form: 1) lateral inflow, L = 0; 2) seepage lateral outflow, L = -0.5qQ/A; and 3) bulk lateral outflow, L = -qQ/A.

Eqs. (51)-(52) which are nonlinear partial differential equations, must be solved by numerical techniques. An implicit 4-pt. finite difference technique is used to obtain a solution to either set of equations. This particular technique (Fread, 1974) is used for its computational efficiency, flexibility, and convenience in the application of the equations to flow in complex channels existing in nature. In essence, the technique determines the unknown quantities (Q and h at all specified cross-sections along the downstream channel-valley at various times into the future; the solution is advanced from one time to a future time by a finite time interval (time step) of magnitude Δt. The flow equations are expressed in finite difference form for all cross-sections along the valley and then solved simultaneously for the unknowns (Q and h) at each cross-section. Due to the nonlinearity of the partial differential equations and their finite difference

representations, the solution is iterative and a highly efficient quadratic iterative technique known as the Newton-Raphson method is used. Convergence of the iterative technique is attained when the difference between successive iterative solutions for each unknown is less than a relatively small prescribed tolerance. Usually, one to three iterations at each time step are sufficient for convergence to be attained for each unknown at all cross-sections. A more complete description of the solution technique may be found elsewhere (Amein and Fang, 1970; Fread, 1974a, Fread, 1977).

3.4 Tributary Inflows/Outflows

Unsteady flows associated with tributaries downstream of the dam can be added to the unsteady flow resulting from the dam failure. This is accomplished via the term q in Eq. (51). The tributary flow is distributed along a single Δx reach. Backwater effects of the dam-break flow on the tributary flow are ignored, and the tributary flow is assumed to enter perpendicular to the dam-break flow. Outflows are assigned negative values. Outflows which occur as broad-crested weir flow over a levee or natural crest may be simulated. The crest elevation, discharge coefficient, and location along the river-valley must be specified. The head is computed as the average water surface elevation, along the length of the crest, less the crest elevation.

3.5 Multiple Dams and Bridges

The dam-break flood forecasting model can simulate the progression of a dam-break wave through a downstream valley containing a reservoir created by another downstream dam, which itself may fail due to being sufficiently overtopped by the wave produced by the failure of the upstream dam. In fact, an unlimited number of reservoirs located sequentially along the valley can be simulated. When the tailwater below a dam is affected by flow conditions downstream of the tailwater section (e.g., backwater produced by a downstream dam, flow constriction, bridge, and/or tributary inflow), the flow occurring at the dam is computed by using an internal boundary condition at the dam. In this method the dam is treated as a short Δx reach in which the flow through the reach is governed by the following two equations rather than either Eqs. (51)-(52):

$$Q_i = Q_{i+1} \tag{55}$$

$$Q_i = Q_b + Q_s \tag{56}$$

in which Q_b and Q_s are breach flow and spillway flow. In this way, the flows Q_i and Q_{i+1} and the elevations h_i and h_{i+1} are in balance with the other flows and elevations occurring simultaneously throughout the entire flow system which may consist of additional dams which are treated as additional internal boundary conditions via Eqs. (55)-(56).

Highway/railway bridges and their associated earthen embankments which are located at points downstream of a dam may also be treated as internal boundary conditions. Eqs. (55)-(56) are used at each bridge; the term Q_s in Eq. (56) is computed by the following expression:

$$Q_s = C\sqrt{2g}\ A_{i+1}(h_i - h_{i+1})^{1/2} + C_d k_s (h - h_c)^{3/2} \quad (57)$$

in which C is a coefficient of bridge flow, C_d is the coefficient of flow over the crest of the road embankment, h_c is the crest elevation of the embankment, and k_s is similar to Eqs. (38)-(39).

3.6 Supercritical Flow

The DAMBRK model can simulate the flow through the downstream valley when the flow is supercritical. This type of flow occurs when the slope of the downstream valley exceeds about 50 ft/mi. Slopes less than this usually result in the flow being subcritical to which all preceding comments pertaining to the downstream routing apply. When the flow is supercritical, any flow disturbances cannot travel back upstream; therefore, the downstream boundary becomes superfluous. Thus, for supercritical flow, a downstream boundary condition is not required; however, an additional equation other than the reservoir outflow hydrograph is needed. To satisfy this requirement, an equation similar to Eq. (40) but with a time-dependent energy slope, is used at the upstream boundary. Multiple reservoirs on supercritical valley slopes must be treated using a storage routing technique such as Eq. (50) rather than the dynamic routing technique.

3.7 Floodplain Compartments

The DAMBRK model can simulate the exchange of flow between the river and floodplain compartments. The floodplain compartments are formed by one or two levees which run parallel to the river on either or both sides of the river, and other levees or road embankments which run perpendicular to the river. Flow transfer between a floodplain compartment and the river is assumed to occur along one Δx reach and is controlled by broad-crested weir flow with submergence correction. Flow can be either away from the river or into the river, depending on the relative water surface elevations of the river and the floodplain compartment. The river elevations are computed via Eqs. (51)-(52), and the floodplain water surface elevations are computed by a simple storage routing relation, i.e.,

$$V_\ell^{\,t} = V_\ell^{\,t-\Delta t} + \left(I^t - O^t\right) \Delta t/43560 \quad (58)$$

in which V_ℓ is the volume (acre-ft) in the floodplain compartment at time t or $t-\Delta t$ referenced to the water elevation, I is the inflow from the river or adjacent floodplain compartments, and O is the outflow from the floodplain compartment to the river and/or to adjacent floodplain compartments. Flow transfer between adjacent floodplain compartments is also controlled by broad-crested weir flow with submergence correction. The broad-crested weir flow is according to the following:

$$I = c\ s_b\ (h_r - h_{fp})^{3/2} \quad (59)$$

$$O = c\, s_b \left(h_{fp} - h_r\right)^{3/2} \tag{60}$$

in which c is a specified discharge coefficient, h_r is the river elevation, h_{fp} is the water surface elevation of the floodplain, and s_b is the submergence correction factor, i.e.

$$s_b = 1.0 \qquad h_r < 0.67 \tag{61}$$

$$s_b = 1.0 - 27.8\left(H_r - 0.67\right)^3 \qquad h_r > 0.67 \tag{62}$$

$$H_r = \left(h_r - h_w\right)/\left(h_{fp} - h_w\right) \tag{63}$$

and h_w is the specified elevation of the crest of the levee. The floodplain elevation $\left(h_{fp}\right)$ is obtained iteratively via a table look-up algorithm from the specified table of volume-elevation values. The outflow from a floodplain compartment may also include that from one or more pumps associated with each floodplain compartment. Each pump has a specified discharge-head relation given in tabular form along with start-up and shut-off operation instructions depending on specified water surface elevations. The pumps discharge to the river.

3.8 Routing Losses

Often in the case of dam-break floods, where the extremely high flows inundate considerable portions of channel overbank or valley flood plain, a measurable loss of flow volume occurs. This is due to infiltration into the relatively dry overbank material, detention storage losses, and sometimes short-circuiting of flows from the main valley into other drainage basins via canals. Such losses of flow may be taken into account via the term q in Eq. (51). An expression describing the loss is given by the following:

$$q_m = -0.00458\, V_L\, P/(L\, \bar{T}) \tag{64}$$

in which V_L is the outflow volume (acre-ft) from the reservoir; P is the volume loss ratio which may range from 0 to as high as 0.3; L is the length (mi) of downstream channel through which the loss occurs; and T is the average duration (hr) of the flood wave throughout the reach length L; and q_m is the maximum lateral outflow (cfs/ft) occurring along the reach L throughout the duration of flow. The mean lateral outflow is proportioned in time and distance along the reach L.

3.9 Landslide Generated Waves

Reservoirs are sometimes subject to landslides which rush into the reservoir displacing a portion of the reservoir contents, and thereby

creating a very steep water wave which travels up and down the length of the reservoir. This wave may have sufficient amplitude to overtop the dam and precipitate a failure of the dam, or the wave by itself may be large enough to cause catastrophic flooding downstream of the dam without resulting in the failure of the dam as perhaps in the case of a concrete dam.

The capability to generate waves produced by landslides is provided within DAMBRK. The volume of the landslide mass, its porosity, and time interval over which the landslide occurs, are input to the model. Within the model, the landslide mass is deposited within the reservoir in layers during small computational time steps, and simultaneously the original dimensions of the reservoir are reduced accordingly. The time rate of reduction in the reservoir cross-sectional area creates the wave during the solution of the unsteady flow Eqs. (51)-(52), which are applied to he cross-sections describing the reservoir characteristics.

3.10 Model Testing

The DAMBRK model has been tested on five historical dam-break floods to determine its ability to reconstitute observed downstream peak stages, discharges, and travel times. Those floods that have been used in the testing are: 1976 Teton Dam, 1972 Buffalo Creek Coal-Waste Dam, 1889 Johnstown Dam, 1977 Toccoa (Kelly Barnes) Dam, and the 1977 Laurel Run Dam floods. However, only the Teton flood will be presented herein.

The Teton Dam, a 300 ft. high earthen dam with a 3,000 ft. long crest, failed on June 5, 1976, killing 11 people making 25,000 homeless, and inflicting about $400 million in damages to the downstream Teton-Snake River Valley. Data from a Geological Survey Report by Ray, et al. (1977) provided observations on the approximate development of the breach, description of the reservoir storage, downstream cross-sections and estimates of Manning's n approximately every 5 miles, indirect peak discharge measurements at three sites, flood peak travel times, and flood peak elevations. The inundated area is shown in Fig. 7.

The following breach parameters were used in DAMBRK to reconstitute the downstream flooding the downstream flooding due to the failure of Teton Dam: τ = 1.25 hrs, BB = 150 ft, z = 0, h_{bm} = 0.0, $h_f = h_d = h_o$ = 261.5 ft. Cross-sectional properties at 12 locations shown in Fig. 7 along the 60 mile reach of the Teton-Snake River Valley below the dam were used. Five top widths were used to describe each cross-section. The downstream valley consisted of a narrow canyon (approx. 1,000 ft. wide) for the first 5 miles and thereafter a wide valley which was inundated to a width of about 9 miles. Manning's n values ranging from 0.028 to 0.047 were provided from field estimates by the Geological Survey. Values of Δx between cross-sections gradually increased from 0.5 miles near the dam, to 1.5 miles near the downstream boundary at the Shelly gaging station (valley mile 59.5 downstream from the dam). The reservoir surface area-elevation values were obtained from Geological Survey topo maps. The downstream boundary was assumed to be channel flow control as represented by a loop rating curve given by Eq. (40).

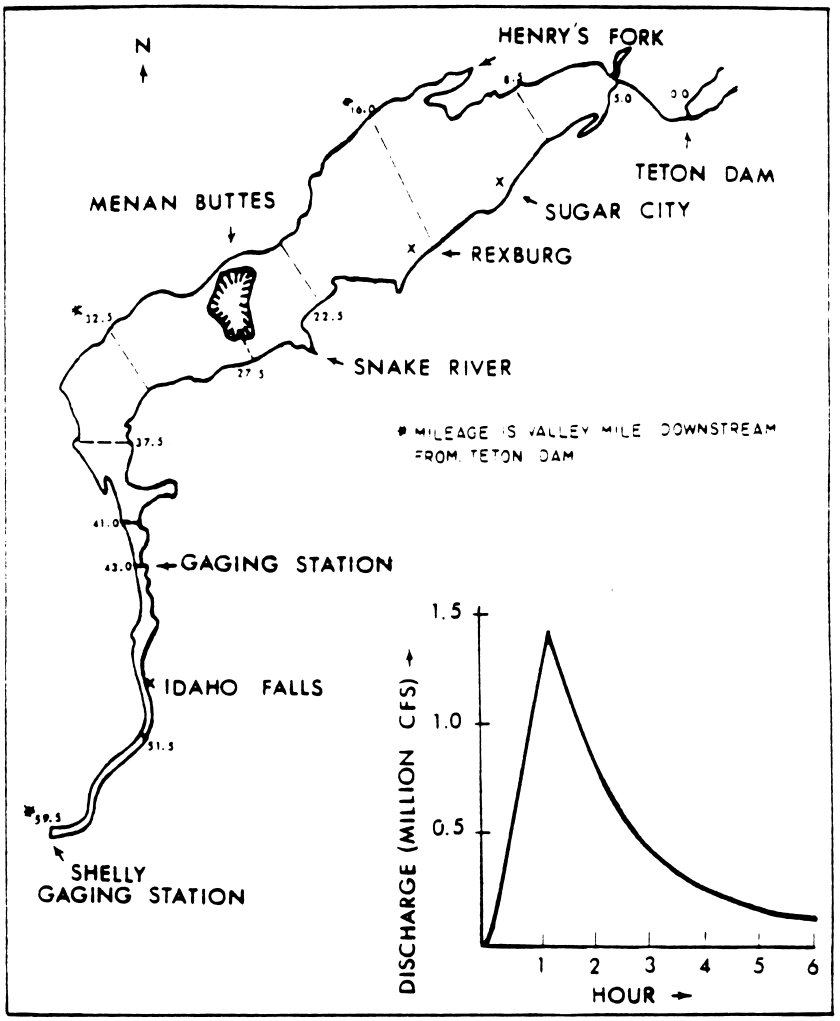

Figure 7. Outflow Hydrograph and Flooded Area Downstream of Teton Dam

The computed outflow hydrograph is shown in Fig. 7. It has a peak value of 1,652,300 cfs (cubic feet per second), a time to peak of 1.25 hrs, and a total duration of about 6 hrs. The peak is about 20 times greater than the flood of record. The temporal variation of the computed outflow volume compared within 5 percent of observed values. The computed peak discharge values along the 60-mile downstream valley are shown in Fig. 8 along with three observed (indirect measurement) values at miles 8.5, 43.0, and 59.5. The average difference between the computed and observed values is 4.8 percent. Most apparent is the extreme attenuation of the peak discharge as the flood wave progresses though the valley. Two computed curves were assumed, i.e., $q_m = 0$; and a second in which the losses were assumed to be uniform along the valley. The losses were assumed to vary from 0 to a maximum of $q_m = -0.30$ and were accounted for in the model through the q term in Eq. (51). Losses were due to infiltration and detention storage behind irrigation levees.

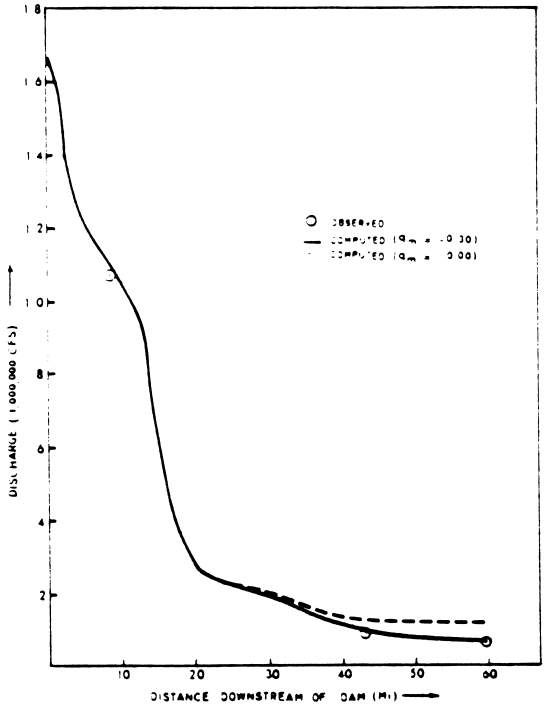

Figure 8. Profile of Peak Discharge from Teton Dam Failure

The a priori selection of the breach parameters (τ and BB) causes the greatest uncertainty in forecasting dam-break flood waves. The sensitivity of downstream peak discharges to reasonable variations in τ and $\bar{b}$ is shown in Fig. 9.

Although there are large differences in the discharges (+45 to -25 percent) near the dam, these rapidly diminish in the downstream direction. After 10 miles the variation is +20 to -14 percent, and after 15 miles the variation has further diminished (+15 to -8 percent). The tendency for extreme peak attenuation and rapid damping of differences in the peak discharge is accentuated in the case of Teton Dam due to the presence of the very wide valley. Had the narrow canyon extended all along the 60-mile reach to Shelly, the peak discharge would not have attenuated as much as the differences in peak discharges due to variations in τ and $\bar{b}$ would be more persistent. In this instance, the peak discharge would have attenuated to about 350,000 rather than 67,000 as shown in Fig. 9, and the differences in peak discharges at mile 59.5 would have been about 27 percent as opposed to less than 5 percent as shown in Fig. 9.

Computed peak elevations compared favorably with observed values. The average absolute error was 1.5 ft, while the average arithmetic error was only -0.2 ft.

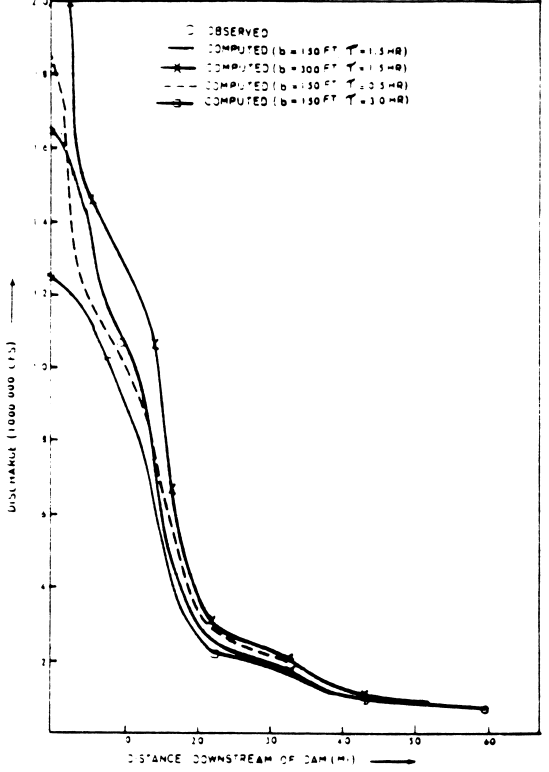

Figure 9. Profile of Peak Discharge from Teton Dam Failure Showing Sensitivity of Various Input Parameters.

The computed flood peak travel times and three observed values are shown in Fig. 10. The differences between the computed and observed are about 10 percent for the case of using the estimated Manning's n values and about 1 percent if the n values are slightly increased by 7 percent.

As mentioned previously, the Manning's n must be estimated, especially for the flows above the flood of record. The sensitivity of the computed stages and discharges of the Teton flood due to a substantial change (20 percent) in the Manning's n was found to be as follows: 1) 0.5 ft. in computed peak water surface elevations or about 2 percent of the maximum flow depths, 2) 16 percent deviation in the computed peak discharges, 3) 0.8 percent change in the total attenuation of peak discharge incurred in the 60-mile reach from Teton Dam to Shelly, and 4) 15 percent change in the flood peak travel time to Shelly. These results indicate that Manning's n has little effect on peak elevations or depths; however, the travel time is affected by nearly the same percent that the n values are changed.

A typical simulation of the Teton flood as described above involved 73 Δx reaches, 55 hrs of prototype time, and an initial time step (Δt) of 0.06 hrs. Such a simulation run required only 19 seconds of CPU time on an IBM 360/196 computer system; the associated cost was less than $5 per run. Microcomputer runs require about 10 min for the Teton simulation.

Information on similar testing of DAMBRK on the Buffalo Creek flood can be found in Fread (1977, 1984a). The results showed a similar degree of comparison between computed and observed values.

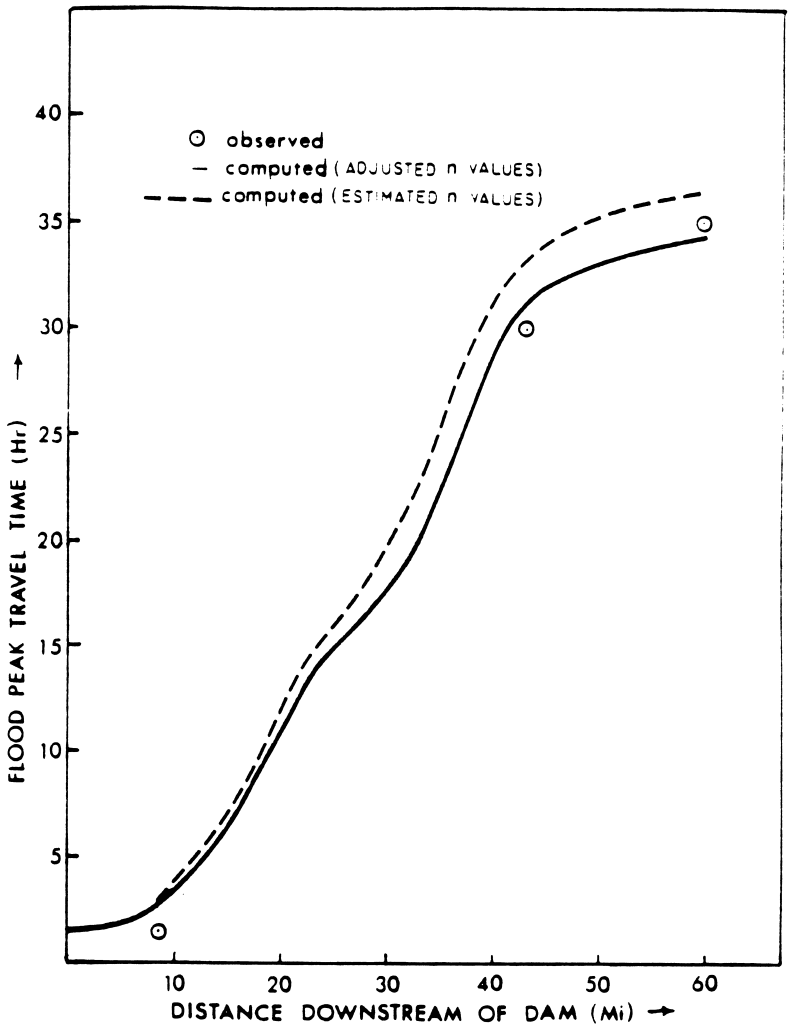

Figure 10. Travel Time of Flood Peak from Teton Dam Failure.

4. SMPDBK

SMPDBK is a simple model for predicting the characteristics of the floodwave peak produced by a breached dam (Wetmore and Fread, 1984). It will, with minimal computational resources (hand-held computers, microcomputers), determine the peak flow, depth, and time of occurrence at selected locations downstream of a breached dam. SMPDBK first computes the peak outflow at the dam, based on the reservoir size and the temporal and geometrical description of the breach. The computed floodwave and channel properties are used in conjunction with routing curves to determine how the peak flow will be diminished as it moves downstream. Based on this predicted floodwave reduction, the model computes the peak flows at specified downstream points. The model then computes the depth reached by the peak flow based on the channel geometry, slope, and roughness at these downstream points. The model also computes the time required for the peak to reach each forecast point and, if a flood depth is entered for the point, the time at which that depth is reached as well as when the floodwave

recedes below that depth, thus providing a time frame for evacuation and fortification on which a preparedness plan may be based. The SMPDBK Model neglects backwater effects created by downstream dams or bridge embankments, the presence of which can substantially reduce the model's accuracy. However, its speed and ease of use together with its small computational requirement make it a attractive tool for use in cases where limited time and resources preclude the use of the DAMBRK Model. In such instances planners, designers, emergency managers, and consulting engineers responsible for predicting the potential effects of a dam failure may employ the model in situations where backwater effects are not significant for pre-event delineation of areas facing danger should a particular dam fail.

4.1 General Description

The SMPDBK model retains the critical deterministic components of the numerical DAMBRK model while eliminating the need for large computer facilities. SMPDBK accomplishes this by approximating the downstream channel as a prism, neglecting the effects of off-channel storage, concerning itself with only the peak flows, stage, and travel times, neglecting the effects of backwater from downstream bridges and dams, and utilizing dimensionless peak-flow routing graphs developed using the NWS DAMBRK model. The applicability of the SMPDBK model is further enhanced by its minimal data requirements; the peak flow at the dam may be calculated with only four readily accessible data values and the downstream channel may be defined by a single "average" cross-section, although prediction accuracy increases with the number of cross-sections specified.

Three steps make up the procedure used in the SMPDBK model. These are: (1) calculation of the peak outflow at the dam using the temporal and geometrical description of the breach and the reservoir volume; (2) approximation of the channel downstream of the dam as a prismatic channel; and (3) calculation of dimensionless routing parameters used with dimensionless routing curves to determine the peak flow at specified cross sections downstream of the dam.

4.2 Breach Description and Peak Outflow Computation

Since earthen dams generally do not fail completely nor instantaneously, the SMPDBK model allows for the investigation of partial failures occurring over a finite interval of time. And, although the model assumes a rectangular-shaped breach, a trapezoidal breach may be analyzed by specifying a rectangular breach width that is equal to the average width of the trapezoidal breach. Failures due to overtopping of the dam and/or failures in which the breach bottom does not erode to the bottom of the reservoir may also be analyzed by specifying an appropriate "H" parameter which is the elevation of the reservoir water surface elevation when breach formation commences minus the final breach bottom elevation (i.e., "H" is the depth to which the breach cuts).

The model uses a single equation to determine the maximum breach outflow and the user is required to supply the values of four variables for this equation. These variables are: 1) the surface area (A_s, acres) of the

reservoir; 2) the depth (H, ft) to which the breach cuts; 3) the time (t_f, minutes) required for breach formation; and 4) the final width (B_r, ft) of the breach. These parameters are substituted into a broad-crested weir flow equation to yield the maximum breach outflow (Q_{bmax}) in cfs, i.e.

$$Q_{bmax} = Q_o + 3.1\ B_r \left(\frac{C}{\frac{t_f}{60} + \frac{C}{\sqrt{H}}}\right)^3 \tag{65}$$

where: $$C = \frac{23.4\ A_s}{B_r} \tag{66}$$

and Q_o is the spillway flow and overtopping crest flow which is estimated to occur simultaneously with the peak breach outflow.

Once the maximum outflow at the dam has been computed, the depth of flow produced by this discharge may be determined based on the geometry of the channel immediately downstream of the dam, the Manning "n" (roughness coefficient) of the channel and the slope of the downstream channel. This depth is then compared to the depth of water in the reservoir to find whether it is necessary to include a submergence correction factor for tailwater effects on the breach outflow (i.e., to find whether the water downstream is restricting the free flow through the breach). This comparison and (if necessary) correction allows the model to provide the most accurate prediction of maximum breach outflow which properly accounts for the effects of tailwater depth downstream of the dam.

The maximum breach outflow must be corrected iteratively for submergence resulting from tailwater effects if the computed maximum outflow stage (h_{max}) is greater than ($0.67\ h_{weir}$) where h_{weir} is the head over the weir (breach) at time t_f as expressed by the following relation:

$$h_{weir} = \left(\frac{C}{\frac{t_f}{60} + \frac{C}{\sqrt{H}}}\right)^2 \tag{67}$$

where C is defined by Eq. (66).

If the ratio of (h_{max}/h_{weir}) is greater than 0.67, a submergence correction factor must be computed as follows:

$$K_s^* = 1 - 27.8 \left[\frac{h_{max}}{h_{weir}} - 0.67\right]^3 \tag{68}$$

This value for K_s^* is substituted into Eq. (69) to obtain an <u>averaged</u> submergence correction factor given by the following:

$$K_s^k = \frac{K_s^* + K_s^{k-1}}{2} \tag{69}$$

where the k superscript is the iteration counter and the first iteration value for K_s^o is 1. This correction factor is applied to the breach outflow as follows

$$Q_b^k = K_s^k \; Q_b^{k-1} \tag{70}$$

where: $Q_b^{k-1} = Q_{bmax}$ is the first iteration. The corrected breach outflow (Q_b^k) is then used to compute an outflow depth (h_{max}^k). The computation of h_{max} is described later via Eq. (75). Also, because there is decreased flow through the breach, there is less drawdown. Thus, the head over the weir (h_{weir}) must be recalculated using the relation:

$$h_{weir}^k = h_{weir}^{k-1} + \left(Q_b^{k-1} - Q_b^k\right) \frac{t_f \text{ (sec.)}}{2A_s \text{ (sq.ft.)}} \tag{71}$$

Now the ratio of the two new values, h_{max}^k / h_{weir}^k is used in Eq. (68) to compute a new submergence correction factor. If the new maximum breach outflow computed via Eq. (70) is significantly different (± 5%) from that computed in the previous iteration, the procedure is repeated. Generally, within two or three iterations the K_s value will converge and a suitable value for the maximum breach outflow (Q_b) is achieved which properly accounts for the effects of submergence.

4.3 Channel Description

The river channel downstream of the dam to the specified routing point is approximated as a prismatic channel by defining a single cross-section (an average section that incorporates the geometric properties of all intervening sections via a distance weighting technique) and fitting a mathematical function that relates the section's width to depth. This prismatic representation of the channel allows easy calculation of flow area and volume in the downstream channel which is required to accurately predict the amount of peak flow attenuation.

Approximating the channel as a prism requires three steps. First, topwidth vs. depth data must be obtained from topographic maps or survey notes. For each depth (h_i), a distance weighted topwidth $\bar{B}_i$ is defined producing a table of values that may be used for fitting (using least-squares or a log-log plot) a single equation of the form $\bar{B} = \bar{K}h^{\bar{m}}$ to define the prismatic channel geometry. The fitting coefficients ($\bar{K}$ and $\bar{m}$) are computed using the following least squares algorithm:

$$\bar{m} = \frac{\sum [(\log h_i)\ (\log \bar{B}_i)] - \frac{(\sum \log h_i)\ (\sum \log \bar{B}_i)}{I}}{\sum (\log h_i)^2 - \frac{(\sum \log h_i)^2}{I}} \quad (72)$$

$$\log \bar{K} = \frac{\sum \log \bar{B}_i}{I} - \bar{m}\ \frac{\sum \log h_i}{I} \quad (73)$$

$$\bar{K} = 10^{(\log \bar{K})} \quad (74)$$

After computing $\bar{K}$ and $\bar{m}$, the depth (h) may be computed for a given discharge (Q) by using the Manning equation, i.e.,

$$h = (Q/a)^b \quad (75)$$

where: $$a = \frac{1.49}{n} S^{1/2} \frac{\bar{K}}{(\bar{m}+1)^{5/3}} \quad (76)$$

$$b = 3/(3\bar{m}+5) \quad (77)$$

Also, S is the channel bottom slope (ft/ft), and n is the Manning n appropriate for the section of river-valley associated with the computed depth (h). In this manner h_{max} of Eq. (68) can be computed if Q_{bmax} is substituted for Q and the fitting coefficients $\bar{K}$ and $\bar{m}$ apply only to the tailwater section.

4.4 Downstream Routing

The peak outflow discharge determined in the preceding step may be routed downstream using the dimensionless routing curves. (See Fig. 11-13.) These curves were developed from numerous executions of the NWS DAMBRK Model and they are grouped into families based on the Froude number associated with the floodwave peak, and have as their X-coordinate the ratio of the downstream distance (from the dam to a selected cross-section) to a distance parameter (X_c). The Y-coordinate of the curves used in predicting peak downstream flows is the ratio of the peak flow at the selected cross section to the computed peak flow at the dam. To determine the correct family and member curve that most accurately predicts the attenuation of the flood, certain routing parameters must be defined.

The distinguishing characteristic of each curve family is the Froude number developed as the floodwave moves downstream. The distinguishing characteristic of each member of a family is the ratio of the volume in the reservoir to the average flow volume in the downstream channel. Thus it may be seen that to predict the peak flow of the floodwave at a downstream

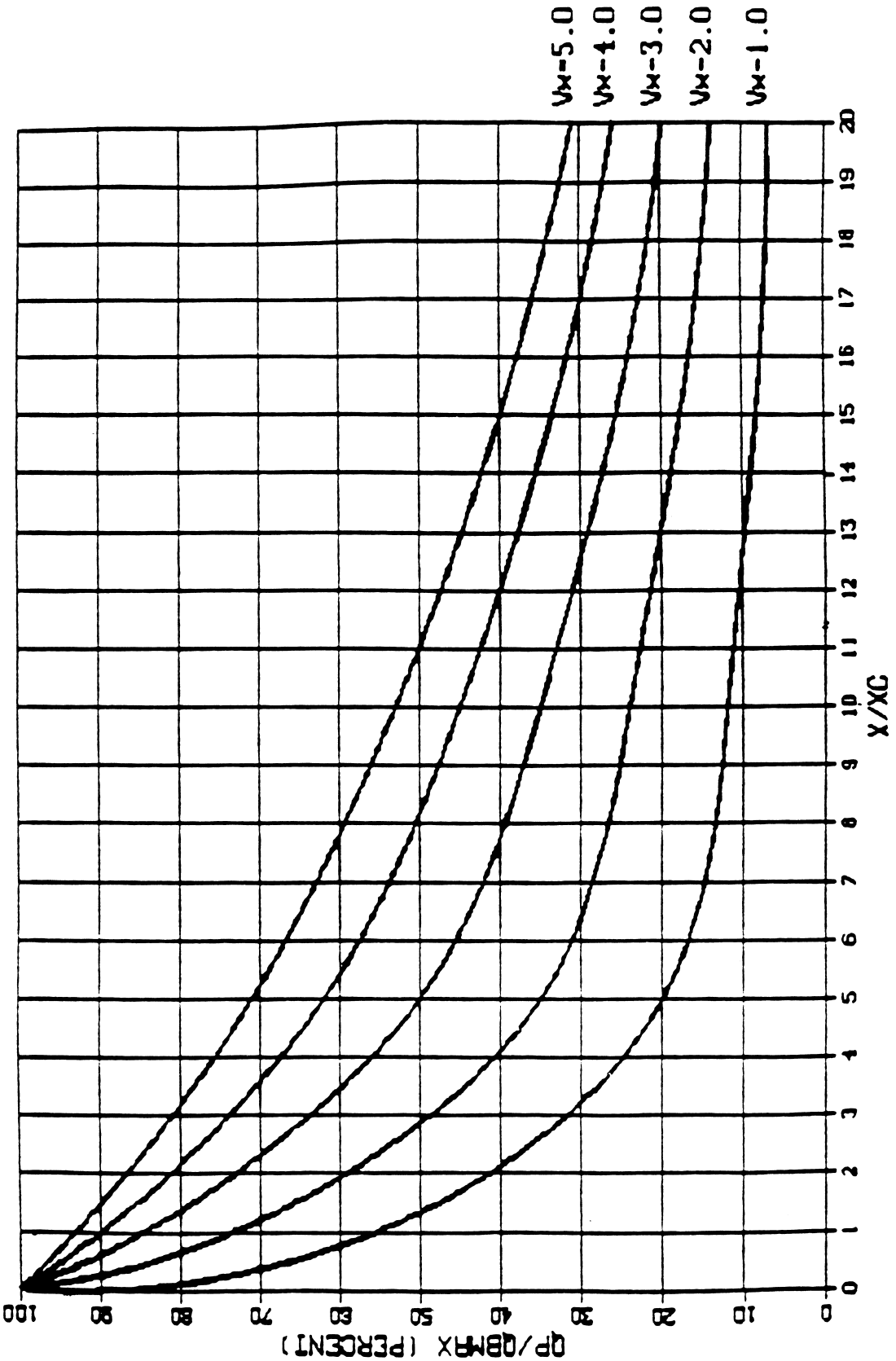

Figure 11. Simplified Routing Curves for F_c = 0.25.

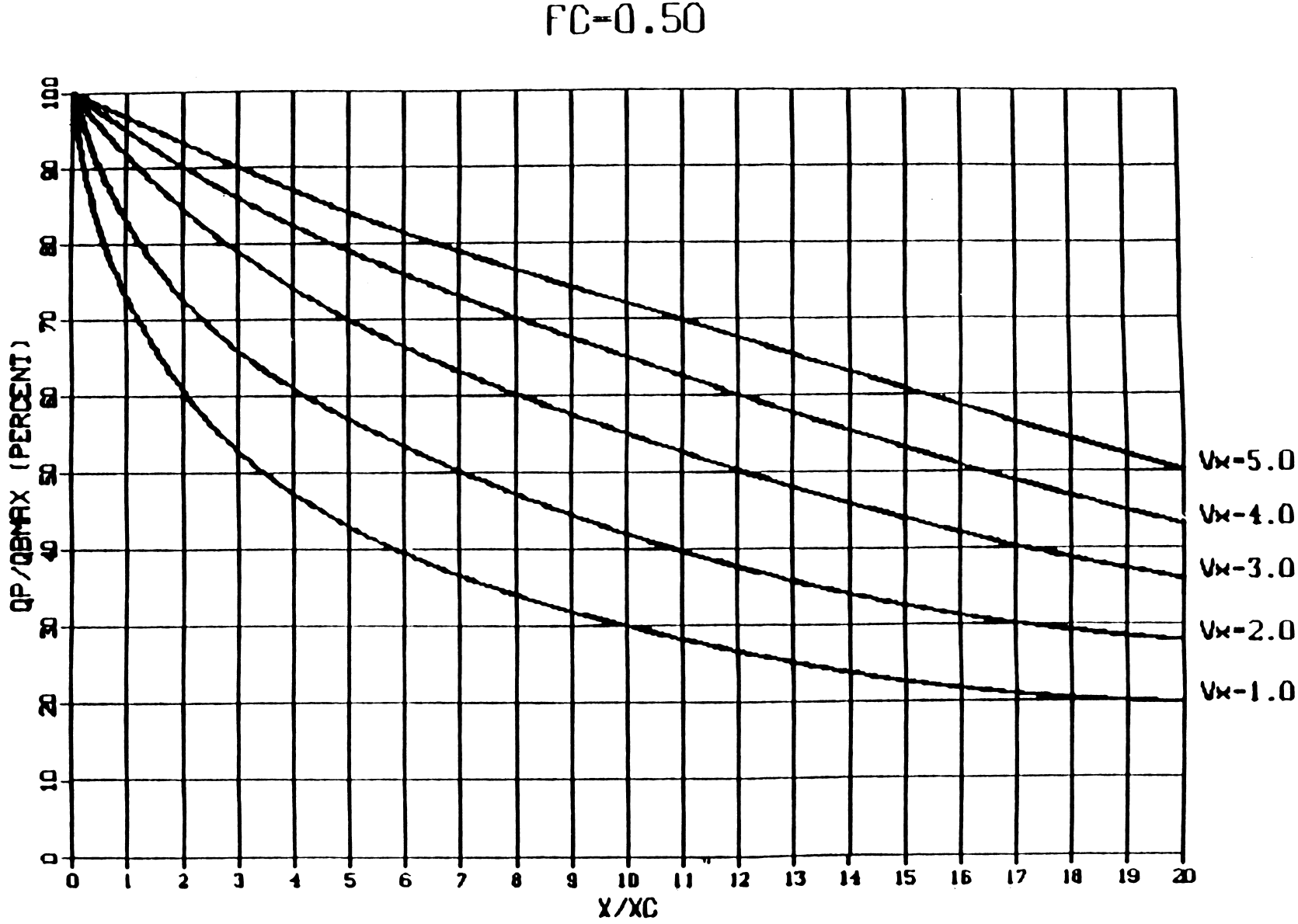

Figure 12. Simplified Routing Curves for F_c = 0.50.

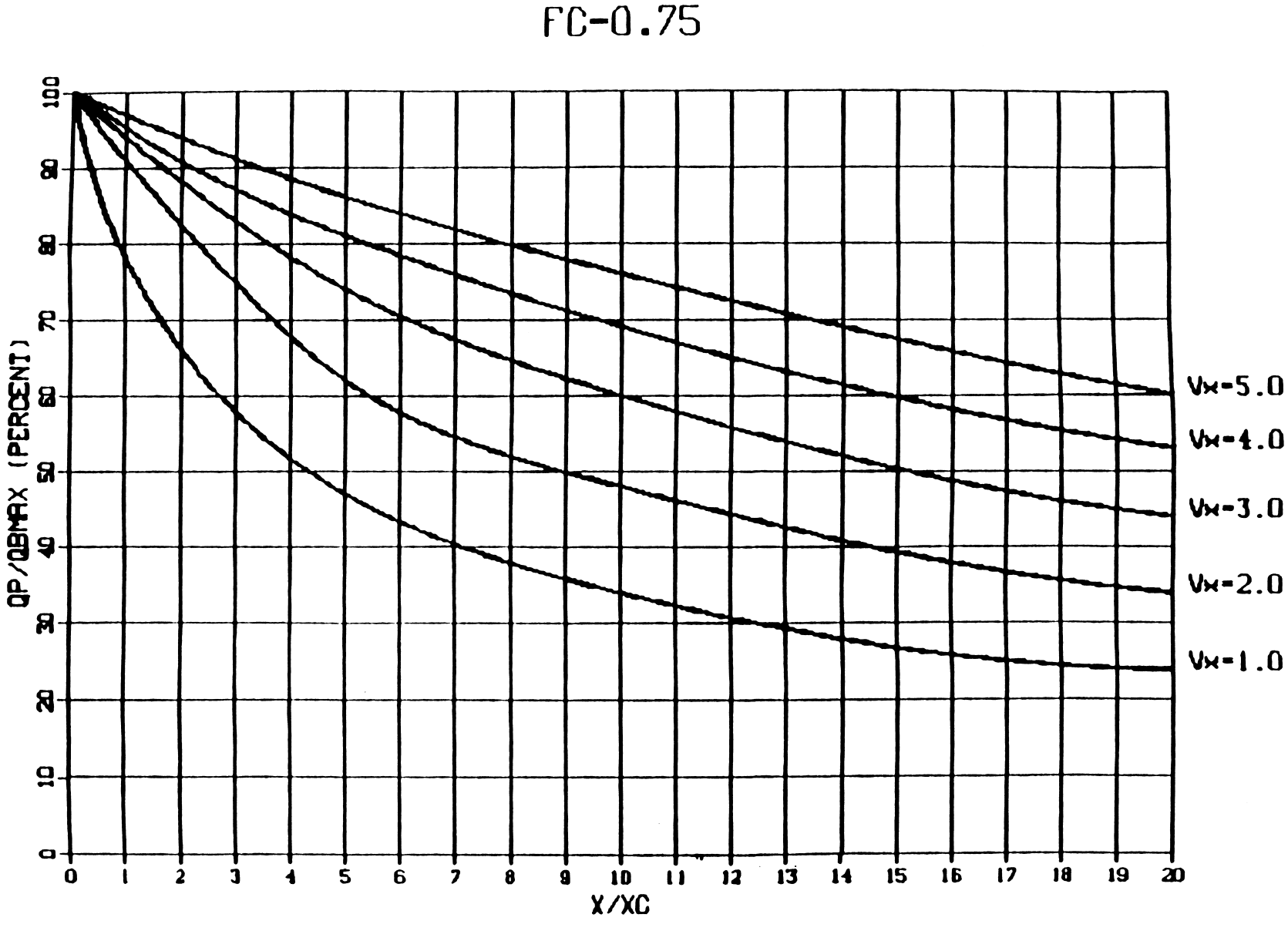

Figure 13. Simplified Routing Curves for F_c = 0.75.

point, the desired distinguishing characteristic of the curve family and member must be determined. This determination is based on the calculation of the Froude number and the volume ratio parameter. To specify the distance in dimensionless form, the distance parameter must also be computed.

The distance parameter (X_c) is calculated using Eq. (78) as follows:

$$X_c \text{ (ft)} = \frac{(\bar{m}+1)}{\bar{K}} \frac{VOL_r}{H_d^{\bar{m}+1}} \frac{6}{1 + 4\ (0.5)^{\bar{m}+1}} \tag{78}$$

where: VOL_r = volume in reservoir (cubic ft)

$\bar{K}$ & $\bar{m}$ = average channel geometry fitting coefficients

H_d = height of dam (ft)

Within the distance (X_c) in the downstream reach, the floodwave attenuates such that the depth at point X_c is h_x (see Fig. 14), which is a function of the maximum depth (h_{max}). The average depth ($\bar{h}$) in this reach is:

$$\bar{h} = \frac{h_{max} + h_x}{2} = \theta\, h_{max} \tag{79}$$

where θ is an empirical weighting factor that must be determined iteratively. The starting estimate for θ is 0.95.

The average hydraulic depth (D_c) in the reach is given by Eq. (80) as follows:

$$D_c = \frac{\theta\, h_{max}}{m+1} \tag{80}$$

The average velocity in the reach is given by the Manning equation, i.e.,

$$V_c = \frac{1.49}{n} S^{1/2} (D_c)^{2/3} \tag{81}$$

where S is the slope of the channel from the dam to the routing point.

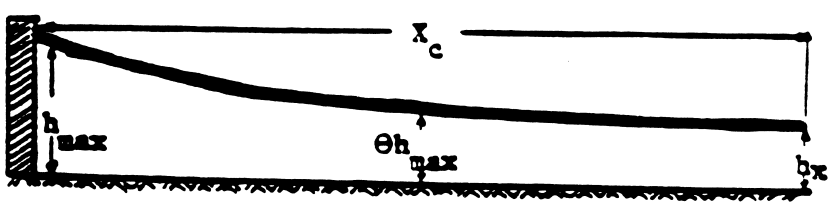

Figure 14. Attenuation of depth downstream of dam.

The average velocity (V_c) and hydraulic depth (D_c) are substituted into Eq. (82) to determine the average Froude number (F_c) in the reach as follows:

$$F_c = \frac{V_c}{\sqrt{gD_c}} \tag{82}$$

where: $g = 32.2$ ft/sec^2 (acceleration of gravity).

The dimensionless volume parameter (V*) that identifies the specific member of the curve family for the computed Froude number is the ratio of the reservoir storage volume to the average flow volume within the X_c reach. The average cross-sectional area of flow (A_c) is given by Eq. (83) as follows:

$$A_c = \bar{K}(\theta h_{max})^{\bar{m}} D_c \tag{83}$$

The volume parameter (V*) is determined by dividing the average flow volume ($A_c X_c$) into the reservoir storage volume (VOL_r), i.e.,

$$V^* = \frac{VOL_r}{A_c X_c} \tag{84}$$

With the values of F_c and V*, the specific curve (Fig. 11-13) can be used (interpolation may be necessary) to determine the routed discharge. The ordinate of the routing curve at $X^* = 1$ is the ratio of the peak flow (Q_p) at X_c to $Q_{b_{max}}$. Knowing Q_p, the stage (h_x) at X_c may be determined using Eq. (75) with the average channel fitting coefficients. The value of θ is checked by rearranging Eq. (79), i.e.,

$$\Theta = \frac{h_{max} + h_x}{2\, h_{max}} \tag{85}$$

If there is a significant difference in the new value of θ from the initial estimate of θ (e.g., ±5%), Eqs. (80)-(84) are recalculated and the new value of θ rechecked. Generally, within two iterations the value for θ will converge.

The distance(s) downstream to the forecast point(s) are non-dimensionalized using the following:

$$X_i^* = \frac{X_i}{X_c} \tag{86}$$

where X_i is the downstream distance to the i^{th} forecast point, i = 1,2,3,...The peak flow at X_i is determined from the proper family of routing curves and the ordinate of the specific V* curve at X_i^*. Multiplying the

value of this ordinate by $Q_{b_{max}}$ produces the peak flow (Q_p) at X_i miles downstream of the dam.

The time of occurrence of the peak flow at a selected cross section is determined by adding the time of failure to the peak travel time from the dam to that cross-section. The travel time is computed using the kinematic wave velocity which is a known function of the average flow velocity throughout the routing reach. The times of first flooding and "de-flooding" of a particular elevation at the cross section may also be determined.

The time of travel for the floodwave to X_i is computed by first calculating the reference flow velocity at the midpoint between the dam and X_i. The user must determine, from the routing curve, the peak flow ($Q_{x/2}$) at ($X_i/2$) miles downstream of the dam. This flow is multiplied by the factor ($0.3 + \bar{m}/10$) and substituted into Eq. (87) to find the reference depth (h_{ref}). Thus,

$$h_{ref} = \left(\frac{Q}{a}\right)^{b} \tag{87}$$

The reference hydraulic depth is given by Eq. (88), i.e.,

$$D_{x_i} = \frac{h_{ref}}{m+1} \tag{88}$$

The reference flow velocity (V_{x_i}) in ft/sec is given by the Manning equation, i.e.,

$$V_{x_i} = \frac{1.49}{n} S^{1/2} \quad D_{x_i}^{2/3} \tag{89}$$

This value for V_{x_i} is substituted into the wave celerity equation (Eq. (90)) to find the wave speed (c) in mi/hr, i.e.,

$$C = 0.682\ V_{x_i} \quad \left[5/3 - 2/3\ \left(\frac{\bar{m}}{\bar{m}+1}\right)\right] \tag{90}$$

The time to peak is then given by Eq. (91) as follows:

$$t_{p_i} = t_f + \frac{X_i}{C} \tag{91}$$

where: t_p = time (hr) of peak occurrences

t_f = time (hr) of failure for dam

To compute the peak depth at mile X_i, K and m coefficients are fitted for that cross-section by substituting the specific depths and topwidths at

mile X_i into Eqs. (72)-(74). Eq. (75) is used to find the peak depth (h_{x_i}) at mile X_i.

The SMPDBK allows the option to determine the time at which flooding commences and/or the time at which it ceases. To do this, a flow rate (Q_f) that corresponds with flood depth at the cross-section is computed as follows:

$$Q_f = a\ h_f^{\ b} \tag{92}$$

where: h_f = flood depth
and a and b are defined by Eqs. (76)-(77) using the K and m coefficients fitted for the cross-section at mile X_i.

This value for Q_f is substituted into Eq. (93) to determine the time to flooding (t_{fld}) as follows:

$$t_{fld} = t_{p_i} - \left(\frac{Q_{p_i} - Q_f}{Q_{p_i} - Q_o}\right) t_f \tag{93}$$

where: t_{p_i} = the time (hr) to peak calculated in Eq. (91)
t_f = the time (hr) of failure for the dam, and
Q_o = the flow (spillway/turbine/overtopping) other than flow.

To determine the time flooding ceases, t_d, the value of Q_f is substituted into the following relation:

$$t_d = t_{p_i} + \left(\frac{24.2\ VOL_r}{Q_{p_i} - Q_o} - t_f\right) \left(\frac{Q_{p_i} - Q_f}{Q_{p_i} - Q_o}\right) \tag{94}$$

where: VOL_r = the reservoir storage volume (ac-ft).

To route the peak flow downstream to cross-sections 3,4,..., the distance-weighted average cross-section must be determined between the dam and the routing point and new $\bar{K}$ and $\bar{m}$ parameters must be fitted to this average cross section. The distance-weighted average cross section may be determined as follows:

For each depth (h_i), the distance weighted topwidth ($\bar{B}_i$) is given by the relation:

$$\bar{B}_i = \frac{\frac{(B_{i,1} + B_{i,2})}{2}(X_2 - X_1) + \ldots + \frac{(B_{i,J-1} + B_{i,J})}{2}(X_J - X_{J-1})}{(X_J - X_1)} \tag{95}$$

where: h_i = the i^{th} depth, i = 1,2,3 ... I (number of topwidths per cross-section

$B_{i,j}$ = the i^{th} topwidth (corresponding to the i^{th} depth h_i) at the j^{th} cross-section where j = 1,2,3, ... J (number of cross-sections)

$\bar{B}_i$ = the weighted i^{th} topwidth

X_j = the downstream distance to the j^{th} cross-section.

The table of values produced by defining a distance-weighted topwidth ($\bar{B}_i$) for each depth (h_i) may then be used for fitting a single equation of the form $B = \bar{K}h^{\bar{m}}$ to define the prismatic channel geometry. The fitting coefficients $\bar{K}$ and $\bar{m}$ may be computed using the least squares algorithm given in Eqs. (72)-(74).

With these weighted average $\bar{K}$ and $\bar{m}$ coefficients, the peak depth is recomputed at the dam using new routing parameters from Eqs. (79)-(84). The flow may then be routed to cross-section 3,4,.... by following the procedure given above.

4.5 Model Testing and Limitations

In both real-time forecasting and disaster preparedness planning, there is a clear need for a fast and economical method of predicting dam-break floodwave peak stages and travel times. The SMPDBK model fills this need, producing such predictions quickly, inexpensively and with reasonable accuracy. For example, in test analyses of the Teton and Buffalo Creek dam failures where the progression of the floodwave was not affected by backwater, approximating the channel as a prism, calculating the maximum breach outflow and stage at the dam, defining the routing parameters, and evaluating the peak stage and travel time to the forecast points required less than 20 minutes of time with the aid of a non-programable hand-held calculator while the average error in forecasted peak flow and travel time was 10-20% with stage errors of approximately 1 ft. Furthermore, comparisons of SMPDBK model results with DAMBRK model results from test runs of theoretical dam breaks show the simplified model produces average errors of 10% or less. The authors had the advantages, however, of prior experience with the model and possession of all required input data, the collection of which consumes precious warning response time in a dam-break emergency.

The SMPDBK Model can be a very useful tool in preparing for and during a dam failure event, however, the user must keep in mind the model's limitations (Fread 1981). First of all, as with all dam breach flood routing models, the validity of the SMPDBK model's prediction depends upon the accuracy of the required input data. To produce the most reliable results, the user should endeavor to obtain the best estimates of the various input parameters that time and resources allow. Secondly, because the model assumes normal, steady flow at the peak, the backwater effects created by downstream channel constrictions such as bridge embankments or

dams cannot be accounted for and the model will predict peak depths upstream of the constriction that may be substantially lower than those actually encountered, while peak depths downstream of the constriction may be over predicted. Finally, because the "slowing down" of the floodwave caused by temporary off-channel dead storage is not accounted for by the model, the predicted time to peak at a certain point may be somewhat shorter than the actual time to peak. Recognizing these limitations and exercising good engineering judgment, the SMPDBK model may provide useful dam break flood inundation information with relatively small expense of time and computing resources.

5. SUMMARY AND CONCLUSIONS

Three NWS models for predicting the flooding due to dam failures were presented. The Breach Model can aid the hydrologist/engineer in determining the properties of the piping or overtopping initiated breach of an earthen dam. This information can be used in conjunction with historical breach data to create the dam breach hydrograph and route it through the downstream channel-valley using the complex DAMBRK Model or the simplified SMPDBK Model. The choice of either the DAMBRK or SMPDBK model is influenced by the available time, data, computer facilities, modeling experience, and required accuracy for each dam break analysis. Complexities in the downstream channel valley such as highway/railway embankment-bridges, significant channel constrictions, levee overtopping, flow volume losses, downstream dams, weirs, lakes require the DAMBRK Model to be used rather than the SMPDBK Model since latter model ignores such factors.

Notwithstanding the capabilities of state-of-the-art models (BREACH, DAMBRK, SMPDBK) the accuracy of the predicted magnitude and timing of downstream flood inundation can be subject to significant error (two feet or more in the crest profile) due to inaccuracies in the following: 1) the reservoir inflow computed from hydrologic precipitation-runoff models; 2) the breach characteristics; 3) the downstream cross-section properties; 4) the estimated flow resistance coefficients; 5) the neglected effects of transported debris of flow resistance and blockage of constricted cross sections; 6) the neglected infiltration and detention storage losses of flood volume; 7) the neglected sediment transport effects on bottom elevation and flow resistance of the downstream channel-flood plain and 8) the highly turbulent flows and complex flow patterns not adequately described by one-dimensional flow equations.

6. REFERENCES

Amein, M., and C.S. Fang, 1970. Implicit flood routing in natural channels. Journal of Hydraulics Division, ASCE, 96, HY12, December, pp. 2481-2500.

Blanton, J.O. III, 1977. Flood plain inundation caused by dam failure. Proceedings of the Dam-Break Flood Routing Workshop, Water Resources Council, pp. 47-64.

Brown, R.J., and D.C. Rogers, 1977. A simulation of the hydraulic events during and following the Teton Dam failure. Proceedings of the Dam-Break Flood Routing Workshop, Water Resources Council, pp. 131-163.

Chow, V.T., 1959. Open-Channel Hydraulics. McGraw-Hill Book Co., New York, pp. 179-188.

De Saint-Venant, Barre, 1871. Theory of unsteady water flow, with application to river floods and to propagation of tides in river channels. Acad. Sci. (Paris) Comptes rendus, 73, pp. 237-240.

Fread, D.L., and T.E. Harbaugh, 1973. Transient hydraulic simulation of breached earth dams. Journal of Hydraulics Division, ASCE, 99, HY1, January, pp 139-154.

Fread, D.L., 1974a. Numerical properties of implicit four-point finite difference equations of unsteady flow. NOAA Tech. Memo. NWS HYDRO-18, U. S. Dept of Commerce, NOAA, National Weather Service, 38 pp.

Fread, D.L., 1974b. Implicit dynamic routing of floods and surges in the Lower Mississippi. Presented at AGU National Meeting, Washington, D. C., April, 26 pp.

Fread, D.L., 1976. Flood routing in meandering rivers with flood plains. Proceedings, Rivers '76, Third Annual Symposium of Waterways, Harbors and Coastal Eng. Div., ASCE, Vol. I, August, pp. 16-35.

Fread, D.L., 1977. The development and testing of a dam-break flood forecasting model. Proceedings of the Dam-Break Flood Routing Workshop, Water Resources Council, pp. 164-197.

Fread, D.L., 1980. Capabilities of NWS model to forecast flash floods caused by dam failures. Proceedings of the Second Conference on Flash Floods, American Meteorological Society, pp. 171-178.

Fread, D.L., 1981. Some limitations of dam breach flood routing models. Preprint, ASCE Fall Convention, St. Louis, Missouri, October 26-30, 1981.

Fread, D.L., 1984a. DAMBRK: The NWS dam-break flood forecasting model. Hydrologic Research Laboratory, National Weather Service, Silver Spring, Maryland, 56 pp.

Fread, D.L., 1984b. A breach erosion model for earthen dams. Proceedings of the Specialty Conference on Delineation of Landslide, Flash Flood, and Debris Flow Hazards in Utah, 30 pp., Utah State University, Logan, Utah.

Johnson, F.A., and P. Illes, 1976. A classification of dam failures. Water Power and Dam Construction, December, pp. 43-45.

Lee, K.L., and J.M. Duncan, 1975. Landslide of April 25, 1974 on the Mantaro River, Peru. National Academy of Sciences, Washington, D.C., 72 pp.

Middlebrooks, T.A., 1952. Earth-dam practice in the United States. Centennial Transactions, ASCE, Paper No. 2620, pp. 697-722.

Morris, H.M., and J.M. Wiggert, 1972. Applied Hydraulics in Engineering. The Ronald Press Co., New York, pp. 69-70, 290, 451-452, 460.

Ponce, V.M., and A.J. Tsivoglou, 1981. Modeling of gradual dam-breaches. Journal of Hydraulics Division, American Society of Civil Engineers, 107(HY6), pp. 829-838.

Ray, H.A., L.C. Kjelstrom, E.G. Crosthwaite, and W.H. Low, 1976. The flood in southeastern Idaho from Teton Dam failure of June 5, 1976. Open File Report, U.S. Geological Survey, Boise, Idaho.

Smart, G.M., 1984. Sediment transport formula for steep channels. Journal of Hydraulics Division, American Society of Civil Engineers, 110 (No. 3), pp. 267-276.

Spangler, M.G., 1951. Soil Engineering. International Textbook Co., Scranton, Pennsylvania, pp. 321-323.

Venard, J.K., 1954. Elementary Fluid Mechanics. John Wiley and Sons, New York, pp. 312-325.

Wetmore, J.N. and D.L. Fread, 1984. The Simplified Dam Break Flood Forecasting Model for Desk-Top and Hand-Held Microcomputers. Office of Hydrology, National Weather Service, Silver Spring, Maryland.